This is to certify that the

dissertation entitled

PETROGRAPHIC AND GEOCHEMICAL
CHARACTERISTICS OF DOLOMITE TYPES
AND THE ORIGIN OF FERROAN DOLOMITE
IN THE TRENTON FORMATION, MICHIGAN BASIN

presented by

Thomas R. Taylor

has been accepted towards fulfillment
of the requirements for

Doctoral ___ degree in __ Geology __

_____
Major professor

Date __ October 11, 1982 __

0-12771

PETROGRAPHIC AND GEOCHEMICAL CHARACTERISTICS
OF DOLOMITE TYPES AND THE ORIGIN OF FERROAN DOLOMITE
IN THE TRENTON FORMATION, MICHIGAN BASIN

By

Thomas R. Taylor

A DISSERTATION

Submitted to
Michigan State University
in partial fulfillment of the requirements
for the degree of

DOCTOR OF PHILOSOPHY

Department of Geology

1982

ABSTRACT

PETROGRAPHIC AND GEOCHEMICAL CHARACTERISTICS OF DOLOMITE TYPES AND THE ORIGIN OF FERROAN DOLOMITE IN THE TRENTON FORMATION, MICHIGAN BASIN

By

Thomas R. Taylor

The Trenton Formation (Ordovician) has a relatively thin (< 50 feet) "cap" dolomite which occurs along the edges of the Michigan Basin. The cap dolomite can be distinguished from regional, early diagenetic dolomites and epigenetic dolomites on the basis of major and minor element chemistry, oxygen istope ratios, and rock texture. The most noticable chemical characteristic of the cap dolomite is its high concentration of iron (mean mol% Fe CO_3 ≃ 7).

The distribution of the cap dolomite was controlled by the availability of Fe^{2+} which was in turn controlled by the availability of S^{2-}. In the center of the basin, early diagenetic pore fluids were marine with high concentrations of sulfate. Subsequent reduction to sulfide resulted in the precipitation of iron sulfides (pyrite + iron monosulfide) which used up most of the available Fe^{2+}. As a result only small amounts of ferroan dolomite formed. On the periphery of the basin, subareal exposure resulted in the dilution of pore fluids, reducing the amount of total dissolved sulfur. The pore water system was limited in S^{2-} and only a minor amount of iron sulfide (iron monosulfide) formed. Fe^{2+} was then available for the formation of ferroan dolomite.

This model is supported by the following: 1) The contact between Trenton cap dolomite and the overlying Utica Shale is sharp and probably unconformable. In the center of the basin the contact is gradational. 2) The whole rock

concentration of iron in the cap is approximately equal to that in slightly dolomitized equivalent beds in the basin center. 3) Iron sulfides are abundant in the center of the basin and mostly in the form of pyrite. In the cap, iron sulfide is minor and in the form of iron monosulfide.

ACKNOWLEDGEMENTS

TABLE OF CONTENTS

LIST OF FIGURES

LIST OF FIGURES (Continued)

LIST OF TABLES

INTRODUCTION

Current models for dolomitization are based on studies of Recent dolomite sequences which have relatively simple geologic histories. Most ancient dolomites have had a more complex history, many being the result of multiple dolomitization events (Wanless, 1979; Mattes and Mountjoy, 1980). The present study shows that a) dolomite of different origins within the same formation can be distinguished based on their distribution, rock texture, and chemistry and b) there may be a relationship between dolomitization and shale diagenesis during burial and basin subsidence.

Dolomitization in the Trenton Formation (Ordovician, Michigan Basin) is the result of multiple dolomitization events. The amount and distribution of dolomite in the Trenton varies both spatially and stratigraphically (Landes, 1946; Cohee, 1948; Newhart, 1976). Three major types of dolomite are recognized in the Trenton: 1) A "cap" dolomite which is confined to the upper portions of the Trenton and to the perimeter of the basin, 2) "Fracture-related" dolomites which are related to subsurface faults, fractures, and structures, and 3) A "regional" dolomite which is confined to the southwestern and western edge of the basin. These dolomite types can be distinguished from one another based on their textures, major and minor element chemistries, and $\delta^{18}O$ ratios.

This study is primarily concerned with determining the origin and distribution of the cap dolomite and its possible relationship to the overlying Utica Shale. These dolomites are unusual in that they are enriched in iron (approximately 3-13 mol% $FeCO_3$) and high in Mn. This unusual chemistry implies an origin which is different than is envisioned for Recent dolomites.

Ferroan dolomite has been reported in carbonates, shales, and sandstones. In all cases, ferroan dolomite must form under reducing conditions such that Fe^{2+} can concentrate in solution. In carbonates, some authors have attributed ferroan dolomite to epigenetic processes with temperatures near $100^{\circ}C$ (Choquette, 1971; Mossler, 1971; Murata, et al., 1972; Wong and Oldershaw, 1981). Other studies indicate that ferroan dolomite can form at lower temperatures and shallow burial (Dickson and Coleman, 1980; M'Rabet, 1981). Ferroan dolomite is also common in organic-rich argillaceous sediments as concretions, bands and carbonate beds (Curtis, 1977; Irwin, et al., 1977; Irwin, 1980; Matsumoto and Iijima, 1981). These studies indicate that ferroan dolomite begins to form at near surface levels and continues to form with depth. Ferroan dolomite-ankerite has been reported as a cement or replacement in sandstones (Nash and Pittman, 1975; Al-Shaieb and Shelton, 1978; Land and Dutton, 1978; Boles, 1978; Boles and Franks, 1979). Under conditions of deep burial (> 2500 m), illitization of clay minerals in interbedded shales may be the source of iron and magnesium for ferroan dolomite formation in sandstones (Boles, 1978; Boles and Franks, 1979).

It is proposed in this study that, in the Trenton the availability of dissolved sulfide and the precipitation of iron sulfides controlled the distribution of the ferroan cap dolomite. It has long been recognized that iron sulfides exert controls on the precipitation of siderite in iron-rich systems (Garrels and Christ, 1965; Berner, 1964, 1970, 1971, 1981). More recently it has been proposed that a similar relationship exists between iron sulfides and ferroan dolomite (Irwin, et al., 1977; Irwin, 1980).

Baker and Kastner (1981) propose that SO_4^{2-} has an inhibiting effect on the precipitation of dolomite. If this were the case, dolomitization would be favored under reducing conditions in which SO_4^{2-} concentrations are low. The model

presented in this study differs in that although ferroan dolomite precipitates after the removal of sulfate by bacterial sulfate reduction, it is the competition between the sulfide and carbonate systems for the available Fe^{2+} which limits ferroan dolomite formation.

GENERAL DESCRIPTION OF THE MICHIGAN BASIN

The Michigan Basin is a roughly circular, intracratonic basin centered near Saginaw Bay (Figure 1). Subsurface structures are present throughout and generally trend from northwest to southeast. This dominant NW-SE structural trend reflects lines of weakness in the Precambrian basement as evidenced by gravity studies (Hinze and Merritt, 1969; Hinze, et al., 1975).

The rocks filling the basin span most of the Paleozoic with only a small amount of Mesozoic (Jurassic) strata preserved in the basin center. Most lithologies are of shallow marine origin with limestones and dolomites making up approximately 47% of the total; shales and sandstones approximately 41%; and evaporites approximately 12% (Ells, 1969). The presence of thick sequences of marine carbonates suggests that the Michigan Basin was a relatively stable, shallow basin throughout most of the Paleozoic (Fisher, 1969).

During the Middle Ordovician, the Michigan Basin was bounded on the southeast by the Findlay Arch, southwest by the Kankakee Arch, and on the west by the Wisconsin Arch. The Trenton carbonate sequence was deposited during a Middle Ordovician marine transgression. Exposure of the Trenton prior to deposition of the Late Ordovician Utica Shale has been proposed for northern Indiana and southern Michigan where the contact is extremely sharp (Rooney, 1966). In other parts of the basin, particularly in the basin center, the contact between the Utica and Trenton is gradational and interfingering with no evidence of an unconformity.
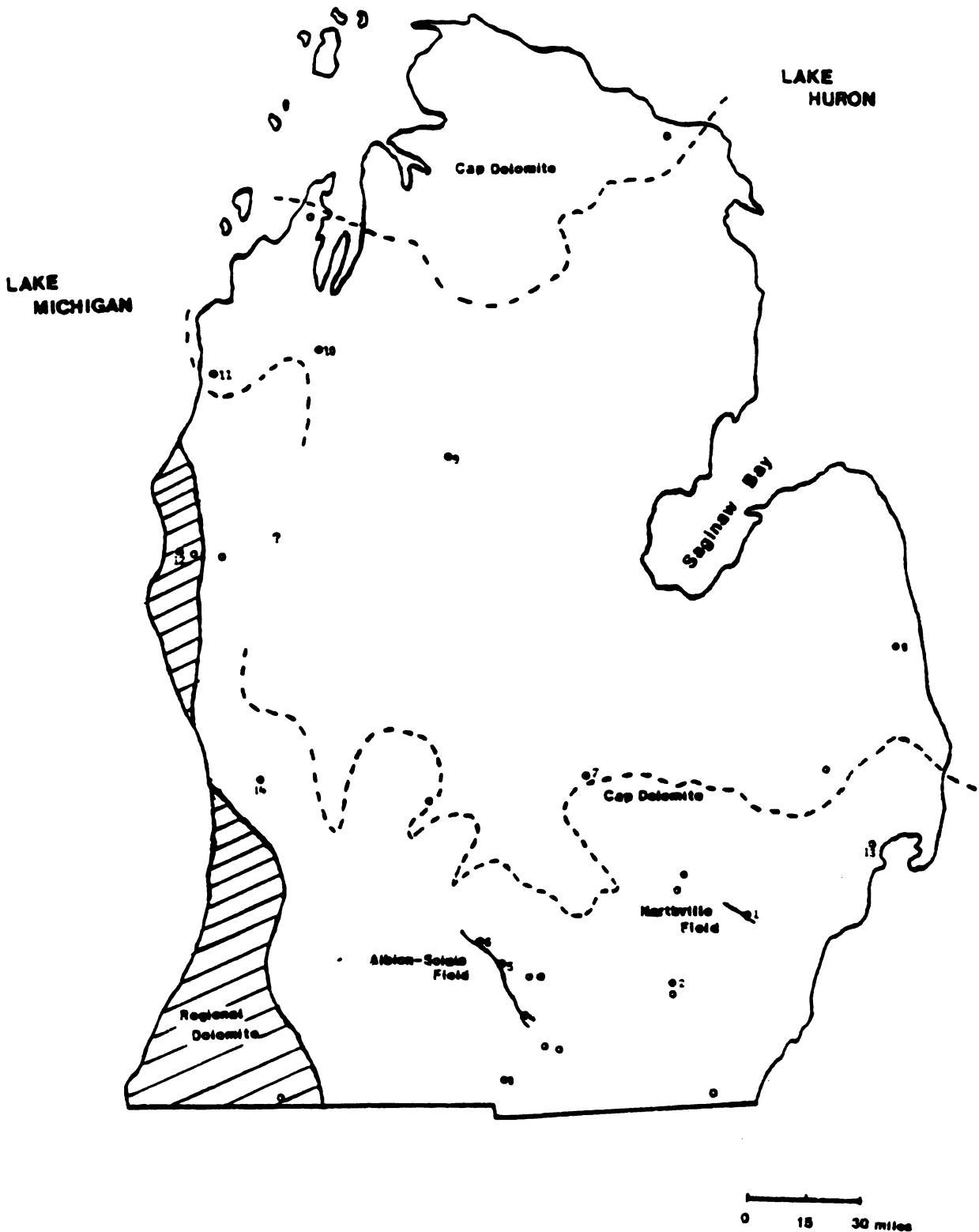
Figure 1. Sketch map of the Michigan Basin showing spatial distribution of major dolomite types and sample locations. The dashed line represents the approximate basinward extent of the cap dolomite. Solid circles are locations of core examined. Open circles are locations of well cutting samples.

Lithologic Description and Depositional Environment

The Trenton Formation is continuous throughout the Michigan Basin and ranges in thickness from 200 to 475 feet (Lilienthal, 1978). Most of the formation consists of a brown to gray, bioturbated, fossiliferous wackestone which is locally rich in argillaceous material. Fossils include echinoderms, brachiopods, trilobites, ostracods, molluscs, bryozoans, and sponges. Grainstone horizons occur periodically throughout the Trenton. The Trenton appears to have been deposited under shallow water, low energy, open marine conditions with occasional storm deposits represented by grainstones (Ardrey, 1978).

The overlying Utica Shale is also continuous throughout the basin but varies in thickness (approximately 100-400 feet). In some areas it thins over Middle Ordovician structures (Nurmi, 1972; Mescher, 1980). The Utica is a black to dark gray calcareous marine shale which becomes more organic-rich near the Trenton contact. Laterally discontinuous laminae of limestone commonly occur in the lower portion of the Utica.

The Trenton Formation does not outcrop in the Southern Peninsula of Michigan. Subsurface core samples from various locations throughout the basin were examined in detail (Figure 1). These cores were chosen on the basis of availability and location. Well cuttings were examined from areas where core was unavailable and used to provide more complete basin coverage.

DISTRIBUTION OF DOLOMITE IN THE TRENTON FORMATION

Three important types of dolomite are recognized in the Trenton and will be referred to as a) cap dolomite, b) regional dolomite, and c) fracture dolomite. The amount of dolomite in the Trenton varies both with depth and position in the basin. This variation forms the basis for separation of Trenton dolomites into three major types.

Cap Dolomites

The upper portion of the Trenton, directly below the Utica Shale, is dolomitized throughout most of the southern part of the basin and in the extreme northern part of the basin (Figure 1). This dolomite unit has been referred to as the cap dolomite (Cohee, 1948). The cap forms a bed of dolomite which has a sharp upper contact with the Utica Shale and grades into limestone at its base. It appears to be continuous in the southern part of the basin but varies in thickness from less than 5 feet up to a maximum of approximately 50 feet. A general thinning of the cap unit toward the basin center is observed. Figure 1 shows the basinward limit of the cap dolomite based on well sample descriptions. Note that no cap dolomite exists in the basin center.

Regional Dolomites

In the extreme western and southwestern parts of the Michigan Basin, the Trenton is, for the most part, completely dolomitized (Cohee, 1948). This type of dolomite is referred to as the regional dolomite and is more extensive with depth than is the cap dolomite. Figure 1 shows the area in which the regional dolomite is encountered. Within this area, the Trenton is either dolomite throughout the section or consists of interbedded dolomite and limestone with dolomite predominating. The regional dolomite unit is correlative with Mid-Ordovician dolomites of Wisconsin.

Fracture-Related Dolomites

The Trenton has been dolomitized along a number of linear fault or fracture zones in the southern part of the basin. The two most extensive examples of these features are the Albion-Scipio and Northville oil fields (Figure 1). Although no significant vertical displacement is recognized in the Trenton, the linear nature and parallel NW-SE orientation of these features, plus

the existence of a gravity anomaly over the Albion-Scipio trend (Hinze, et al., 1975) indicate that basement tectonics may control the location of these fracture zones (Hinze and Merritt, 1969; Hinze, et al., 1975; Shaw, 1975).

The dolomite body associated with these fracture zones can be envisioned as a dolomite dike. The Albion-Scipio dolomite unit is approximately 1 mile wide, 35 miles long, and extends through the Trenton section and much of the Black River Formation. The Northville dolomite unit is approximately ½ mile wide and 6½ miles long with similar vertical extent. The boundaries between the dolomite unit and adjacent limestone are, in many cases, irregular and vary with depth.

Collapse breccias which have subsequently been dolomitized are a common feature in the Albion-Scipio dolomites, indicating that extensive dissolution occurred prior to or contemporaneous with dolomite formation (Shaw, 1975; Ardrey, 1978). The existence of collapse breccia along with the three-dimensional configuration of the dolomite bodies suggests that the fracture zones served as solution pathways along which post-lithification dolomitization occurred.

Other, less extensive occurrences of fracture-related dolomite with textural and chemical characteristics similar to Albion-Scipio and Northville dolomites occur at a number of locations around the basin. Some are smaller scale fracture zones (generally < 1 mile in length) but others appear to be dolomite lenses. Veins of this type of dolomite are also observed. This would indicate that the amount and extent of dolomite formed during this late-stage event is dependent on the development of both large and small scale fractures which serve as solution pathways during dolomitization.

ANALYTICAL METHODS

Major element (Ca, Mg, Fe) and minor element (Na, Mn) analyses of dolomites from the Trenton Formation were performed with the electron microprobe (ARL-EMX-SM). Major element analyses were done with an output voltage of 10KV and beam current of 0.05 microamps. Beam point diameter used for analyses was approximately 3 microns. With the instrument set as described above, five consecutive 20 second analyses produced no systematic variation in count rate and no evidence of sample disintegration. Minor element analyses were done at an output voltage of 12KV and a beam current of 0.10 microamps. This setting was chosen in order to give improved peak to background ratios for Mn and Na without producing sample disintegration. The value of bulk analyses of Na in carbonates has been questioned (M'Rabet, 1981) because much of the Na is present in clays and intergrain residue. Although the electron microprobe may not be as precise as other methods, with this instrument, the operator can avoid such residue and be certain that the Na content of a given grain is being analyzed.

Whole rock iron analyses (reported as wt.%Fe_2O_3) were done by X-ray fluorescence. The method used for these analyses was developed by Reynolds (1963).

Carbon and oxygen isotope analyses for dolomites were run at Amoco Production Research. Samples were attacked for 56 hours with 100% phosphoric acid at $25^{\circ}C$ and the gas analyzed using standard techniques (Sharma and Clayton, 1965; Land, 1981). Calcite analyses were performed at the University of Michigan Stable Isotope Laboratory.

PETROGRAPHY

In addition to the differences in the distribution of dolomite types in the Trenton, there are notable differences in their textures and chemistries. Table 1 summarizes these differences and can be referred to throughout the following discussion.

Cap Dolomites

The Trenton cap dolomite is primarily composed of iron-rich dolomite which stains blue with potassium ferricyanide. The texture of the cap dolomite is typical of many ancient dolomites (Figure 2). The matrix is composed of a fine-grained (0.01-0.10 mm), anhedral, interlocking mosaic of ferroan dolomite. The boundaries between the grains are irregular and numerous stylolites and microstylolites run through portions of the matrix. Fossils are replaced by coarser-grained dolomite (0.2-0.5 mm) with iron contents comparable to the matrix dolomite. Two types of fossil replacement are observed: a) Echinoids are pseudomorphically replaced by single crystals of ferroan dolomite. These crystals contain inclusions which in some cases give some suggestion of the original structure of the fossil (Figure 2a). b) A relatively clear, sparry, anhedral ferroan dolomite with undulose extinction replaced fossils or filled fossil moulds in the upper parts of the Trenton cap (Figure 2b). This dolomite is coarse-grained and appears to have nucleated at the edges of fossils and grown toward the center. Partially replaced fossils are present in some samples. Fossils replaced in this manner are brachiopods, echinoids, and trilobite fragments. Ferroan dolomite with similar undulose extinction is also seen lining voids.

In the lower portions of the cap some samples have a number of fossils which remain as calcite and appear to have resisted dolomitization. Also present

9

Table 1. Summary of textural and chemical differences between Trenton dolomite types.

	Characteristic Texture	$FeCO_3$ %	Mean Mn (ppm)	Mean Na (ppm)	Mean $\delta^{18}O_{PDB}$
Cap Dolomite	-fine-grained, anhedral dolomite matrix -fossils replaced by coarser-grained dolomite	2.15 - 13.41 $\bar{x} = 7.2$	3830	341	-7.7°/oo
Basin Center	-fine-grained, anhedral dolomite matrix -fossils partially or totally replaced by coarse-grained dolomite -abundant Fe-sulfides	3.16 - 13.12 $\bar{x} = 8.33$	5261	411	-7.9°/oo
Fracture-related Dolomite	-coarse-grained, anhedral dolomite -fossils generally not preserved -abundant saddle dolomite	0.03 - 2.3 $\bar{x} = 0.39$	1477	333	-9.0°/oo
Regional Dolomite	-fine-grained, anhedral dolomite matrix -fossils replaced by coarser-grained dolomite	0.4 - 0.41 $\bar{x} = 0.10$	949	425	-6.8°/oo
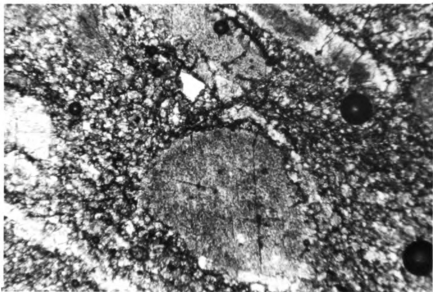
Figure 2a. Texture of ferroan cap dolomite. Note echinoderm replaced by a single dolomite crystal. Width of field = 2.7 mm.
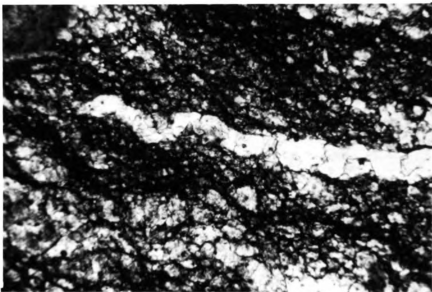
Figure 2b. Brachiopod replaced by crystals of coarse-grained ferroan dolomite. Width of field = 2.7 mm.

are remnants of calcite in partially replaced fossils and some calcite vein fillings.

Iron sulfides (mostly iron-monosulfides, rarely pyrite) are present in trace amounts (generally less than 0.1% of the rock) in the cap dolomite. They occur most often as very minute cubes or irregularly shaped grains and sometimes as framboids. There is a tendancy for iron sulfide to replace fossils although it does occur throughout the dolomite matrix. In most cases, iron sulfide appears to have formed prior to dolomite and is included in individual dolomite crystals (Figure 3). However, in a few cases a later stage of iron sulfide formation is observed. Here iron sulfides are found only between dolomite grains and on the edges of pores, indicating precipitation after dolomitization.

. At the base of the cap unit, within approximately a one-foot interval, the cap dolomite grades into a micritic limestone (biomicrite) with scattered grains of ferroan dolomite. The abundance of dolomite varies with depth. Many of the dolomite grains are rhombic with straight crystal boundaries, particularly those which replace micrite. Most rhombic dolomite grains range in diameter from 0.05 mm to 0.2 mm although some are as course as 0.5 mm. In instances where several rhombs have grown together the grain boundaries are generally irregular. From this relationship it appears that dolomite crystals growing in micrite maintain planar grain boundaries whereas dolomite growing in contact with dolomite results in an irregular grain contact.

Petrographic relations are interpreted as indicating that ferroan dolomite began to form early, at near surface levels but continued to form after lithification and the onset of pressure solution. This implies that formation of the cap dolomite may have been a slow process which occurred over a range of depths and temperatures. Evidence for this is observed in dolomitic limestones directly beneath the cap dolomite. Stylolites are abundant in these rocks and in

Figure 3. Large brachiopod with iron monosulfide in center is partially replaced by coarse-grained ferroan dolomite. Note that iron sulfides are included in dolomite. Width of field = 1.65 mm.

a number of cases ferroan dolomite rhombs are superimposed on the stylolite. Some fossil grains which have clearly undergone pressure solution and volume reduction have dolomite rhombs superimposed on the surface where dissolution has occurred. Also, some microfractures are filled with the same type of dolomite. It is clear from this relationship that ferroan dolomite was forming during and after the onset of pressure solution and therefore after lithification. In some cases, the amount of dolomite increases near stylolites; a relationship which is observed in other ancient limestones (Wanless, 1979). Stylolites and solution seams may have acted as conduits for dolomite forming solutions after lithification. Other relationships between dolomite and stylolites indicate that much of the dolomitization occurred prior to or during pressure solution. These include stylolites which are distorted around and dissolve dolomite grains, stylolites which cut through dolomite grains, and stylolites which separate completely dolomitized rock from partially dolomitized rock.

Basin Center. Trenton core from the central portion of the Michigan Basin (Figure 1, Location 9) contain a small amount of ferroan dolomite. The dolomite has textural characteristics similar to the cap dolomites, however, it does not form a distinct, completely dolomitized unit.

At the Trenton-Utica contact (picked as the first continuous carbonate bed) a one-foot thick band of partially dolomitized limestone (30-80% dolomite) occurs. As in the cap dolomite, the matrix is composed of a very fine-grained (0.01-0.03 mm), equant, ferroan dolomite (Figure 4). The grains are generally anhedral, except where insoluble clays and organic material separate dolomite crystals and allow rhombic faces to persist. In most cases, the matrix is completely dolomitized but in some samples shale layers persist and this fine-grained dolomite occurs in nodules. Portions of the rock are very rich in organic matter.
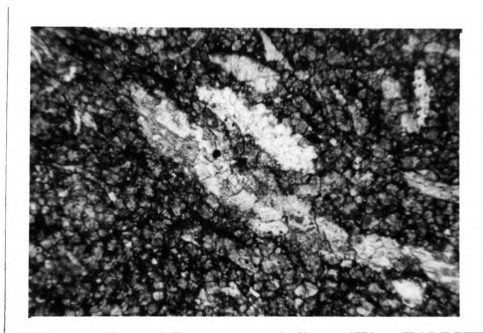
Figure 4. Texture of ferroan dolomite-rich zone in the basin center. Note fine-grained dolomite matrix and coarser-grained fossil replacement. Smaller fossil is calcite. Width of field = 1.65 mm.

Most fossil grains have resisted replacement by dolomite. Those which are dolomitized have been replaced by a coarser-grained (0.15-0.30 mm), anhedral, undulose ferroan dolomite (Figure 4). The same type of undulose dolomite fills or partially fills voids in the rock. Fossil replacing and void filling dolomites with the same features are observed in the cap dolomites.

An important difference between the Trenton in the basin center and the cap dolomites from the southern part of the basin is that iron sulfides are much more abundant in the basin center. In both dolomitized and undolomitized portions of the Trenton, near the contact with the Utica Shale, pyrite and iron-monosulfides are major components of the rock. Point counts give modal iron sulfide from 2 to 10%. Although iron sulfide occurs throughout the rock, bands which are extremely rich in pyrite are common (Figure 5). In these horizons, pyrite may completely replace brachiopods and other fossils. Partially replaced fossils are also commonly observed. In some cases, coarse cubes (0.15-0.2 mm) of pyrite occur both as single, isolated crystals and in association with numerous other pyrite cubes. Very minute iron sulfide crystals occur in fibrous brachiopods and in some instances form framboids. Petrographic evidence for iron sulfides forming before ferroan dolomite is as follows: a) Pyrite cubes are present at the edges of large voids which are now filled with ferroan dolomite. b) Ferroan dolomite grains which partially replace fibrous brachiopods have included minute iron sulfide grains (Figure 3). These minute crystals are also seen in brachiopods which have not undergone partial replacement by ferroan dolomite.

Within approximately 2 feet of the Utica-Trenton contact the amount of ferroan dolomite decreases markedly. At greater than 2 feet below the contact ferroan dolomite is rare and only occurs as a course-grained void lining.
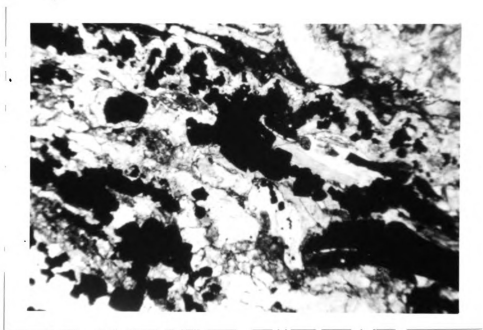
Figure 5. Iron sulfide-rich zone in dolomitic limestone from the basin center. Iron sulfides are a mixture of pyrite and iron monosulfide. Width of field = 2.7 mm.

Regional Dolomite

Dolomites from the western part of the basin differ from the cap dolomite in that they are non-ferroan and form a much thicker sequence of bedded dolomite. The textures observed are similar to the cap dolomite (Figure 6). A fine-grained (0.05-0.15 mm), equant, anhedral matrix of dolomite makes up most of the rock. Fossil forms are recognizable in thin section due to their replacement by a coarser-grained (0.25-0.5 mm), anhedral, clear, non-ferroan dolomite which in some cases has a slightly undulose extinction. Most echinoids are replaced by a single crystal of dolomite and other fossils by a number of crystals. Some appear to have been moulds now filled by clear dolomite. In a few cases, some fossils are preserved as calcite and have resisted dolomitization and/or dissolution. The matrix dolomite has a light brown color in plane light whereas the fossil replacement dolomite is gray or clear, giving the rock a mottled appearance. Iron sulfides are present in very small amounts in some samples. The rock has abundant stylolites and solution seams.

Fracture-Related Dolomite

Dolomites which are related to faults, fractures, and subsurface structures in the Trenton have textures which are distinctly different than the cap dolomites. First of all, fracture dolomites are non-ferroan and coarse-grained xenotopic, with grain diameters ranging from 0.1 mm to 0.5 mm (average $\simeq$ 0.3 mm). The grains form a tight, interlocking mosaic of anhedral, equant dolomite with little or no intercrystalline porosity (Figure 7a). Porosity in these dolomites is in the form of vugs. In contrast to the cap dolomite, fossil grains are not preserved as individual, recognizable units but only occasionally seen as vague ghost fossils. The fracture dolomite grains generally exhibit undulose extinction. Grain centers are cloudy and appear to have abundant micro-inclusions giving the crystals a light brown color in plane light. In some
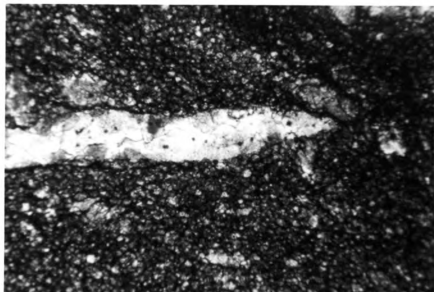
Figure 6. Texture of regional dolomite (non-ferroan). Note similarity of texture with that in Figure 2. Width of field = 2.7 mm.

Figure 7a. Coarse, xenotopic fracture-related dolomite from the Albion-Scipio oil field. Note that fossils are not preserved in this type of dolomite. Width of field = 2.7 mm.

cases clear overgrowths are observed on these grains but in other cases the grains are optically homogeneous. On a hand specimen scale the rock is color mottled with areas of abundant clear overgrowths appearing lighter than areas of dolomite which do not have large clear overgrowths. Thus dolomitization may have occurred in at least two stages.

Sucrosic dolomite occurs at some levels in the Albion-Scipio and Northville Fields (Figure 7b). These are relatively coarse-grained (0.15-0.7 mm), non-ferroan, and have mildly undulose extinction. Zones of inclusion-rich and inclusion free dolomite occur within single crystals. This texture is associated with very high intercrystalline porosity.

The xenotopic dolomite described above is generally vuggy. The vugs are commonly filled or partially filled with a coarse-grained (0.2-3.5 mm), baroque or saddle dolomite with curved crystal faces and broad, sweeping extinction (Figure 7c). Baroque dolomite is non-ferroan and also occurs in veins. This type of dolomite has been described by a number of authors (Choquette, 1971; Folk and Assereto, 1974; Radke and Mathis, 1980) and it has been suggested that its occurrence is indicative of dolomitization at elevated temperatures (Radke and Mathis, 1981).

Relationships Between Dolomite Types: The Order and Timing of Dolomitization

The three major types of dolomite described above represent three distinct and separate events. This is inferred from the textural differences described in the preceeding section and is supported by comparison of their respective chemistries in a later section. Petrographic recognition of the three dolomite types is possible with the use of iron staining techniques combined with comparison of the characteristic textures.

Figure 7b. Sucrosic dolomite zone in fracture dolomite. Dolomite grains have straight crystal boundaries and have inclusion-rich cores. Width of field = 1.65 mm.

Figure 7c. Extremely coarse-grained baroque or saddle dolomite from the Albion-Scipio field. This dolomite occurs as a void filling. Note curved crystal faces and coarse grain size in comparison to dolomite matrix. Width of field = 2.7 mm.

In a number of cores examined in this study, two types of dolomite occur. Detailed petrography of these cores allows the delineation of the order in which the dolomite types formed.

Regional and Cap Dolomites. Although the textures observed in the regional dolomite and cap dolomite are similar, they can be distinguished by staining because the cap dolomites are very rich in iron. Trenton core from the extreme western edge of the basin (Figure 1, Location 12) was examined and the upper 231 feet is composed of regional dolomite. The only ferroan dolomite observed in this core occurs approximately 150 feet from the Trenton top. It is a coarse-grained, void filling baroque dolomite which clearly formed later than regional dolomites (Figure 8). The voids are first lined with a non-ferroan dolomite and in turn followed by ferroan dolomite.

In the cap unit, ferroan dolomite with undulose extinction lines voids now filled with anhydrite. In the basin center, baroque ferroan dolomite, some of which is extremely coarse-grained, is also observed as a void lining and filling. The baroque ferroan dolomite in the core from the western edge of the basin may be a product of the same event which formed baroque ferroan dolomite in other parts of the basin. The regional dolomite, therefore, appears to have formed prior to the ferroan cap dolomite.

Cap and Fracture Dolomites. The cap dolomite and fracture-related dolomite can be distinguished on the basis of both texture and iron content. Cores from the Northville Oil Field (Figure 1, Location 1) and a combination of core and well cuttings from the Albion-Scipio Field (Figure 1, Locations 4, 5, 6) clearly show that the ferroan cap dolomite preceeded the fracture-related dolomite. Other, less extensive occurrences of fracture-related dolomite show the same relationship (Figure 1, Locations 2, 3, 10, 11).
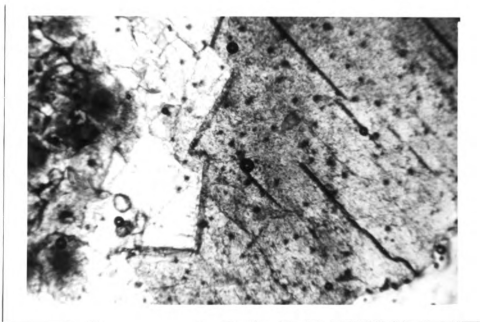
Figure 8. Coarse-grained baroque ferroan dolomite from western Michigan (Location 12, Figure 1). At left is a fine-grained dolomite followed by non-ferroan dolomite lining a void. The void is filled with ferroan dolomite (stained). Width of field = 2.7 mm.

In samples of both the Northville and Albion-Scipio dolomites, non-ferroan overgrowths are observed on ferroan dolomite grains (Figure 9). The contact between the ferroan core and non-ferroan overgrowth is extremely sharp; observed both optically and with the electron microprobe. Therefore, this zoning does not represent a gradual depletion of iron in the pore water system as dolomite formed but instead represents two separate dolomitization events.

The relationship between the cap dolomites and fracture-related dolomites is best seen in three cores from the Northville Field which were examined in detail. These cores were taken slightly off the main fracture zone. Five to ten feet of ferroan cap dolomite is enountered, followed by approximately 100 feet of dolomitic limestone, and approximately 100 feet of fracture-related dolomite. The fact that fracture-related dolomite is encountered at depth, away from the main fracture zone indicates that the width of the fracture dolomite body varies significantly with depth. In samples from the lower portions of the cap, a second phase of dolomite is observed (Figure 9a). It is non-ferroan, clear and has undulose extinction. It most often occurs as overgrowths on pre-existing ferroan dolomite crystals which partially replaced fossils and/or partially filled fossil moulds. This dolomite appears to have replaced remnant calcite and filled open spaces which were left by the ferroan dolomite event. In the matrix, thin overgrowths of non-ferroan dolomite are also observed on some fine-grained ferroan dolomite (Figure 9b). As the cap grades into a dolomitic limestone, rhombs of ferroan dolomite also have non-ferroan overgrowths.

Approximately 120 feet below the base of the cap dolomite a rapid transition to 100% dolomite occurs. The texture of the dolomite is characteristic of the fracture-related dolomite, composed of coarse, xenotopic dolomite and no preservation of fossils. A complex zoning pattern is revealed when the dolomite is stained for iron (Figure 10). Some grains show simple
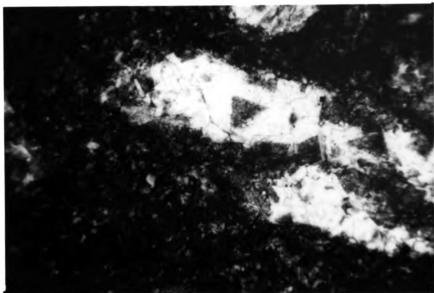
Figure 9a. Ferroan dolomite cores (stained) in dolomite fossil replacement. Non-ferroan, fracture dolomite completed the replacement process. Matrix is fine-grained ferroan dolomite. Width of field = 1.65 mm.
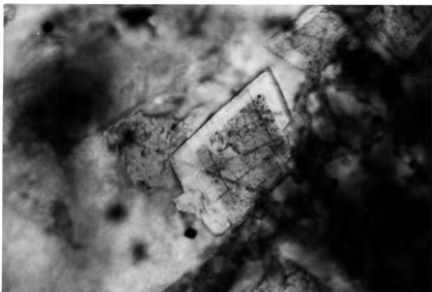
Figure 9b. Non-ferroan dolomite overgrowth on ferroan dolomite core (stained) in the fine-grained dolomite matrix in Figure 9a. Width of field = 0.16 mm.

zoning with ferroan cores and non-ferroan overgrowths (Figure 10a), similar to the zoning seen in samples higher in the section. Another common zoning pattern observed at this level is seen in Figure 10b. The grains have small non-ferroan cores which in many cases have very thin, discontinuous zones of ferroan dolomite within. The cores have an uneven, irregular contact with a relatively thick zone of ferroan dolomite which surrounds it (Figure 10c). This zone is followed by a thick zone of non-ferroan dolomite which is sometimes followed by another ferroan zone. The discontinuous zoning decribed above is confirmed with the microprobe.

The complex zoning pattern described above is interpreted as resulting from the replacement of ferroan dolomite by non-ferroan dolomite. The evidence for this is as follows: a) Very thin, discontinuous zones of ferroan dolomite are preserved in the non-ferroan cores. The discontinuous nature of the ferroan zones is unlikely to occur as a result of crystal growth. b) In zoned crystals, many of the ferroan to non-ferroan zone contacts are irregular. Rarely do non-ferroan cores have rhombic shapes. The irregular shape of these contacts, which is generally convex toward the ferroan zone implies that non-ferroan dolomite was replacing the ferroan dolomite. c) In a number of dolomite grains the outer non-ferroan zone is connected to the non-ferroan cores by a tube of non-ferroan dolomite which cuts through the ferroan zone (Figure 10d). These tubes may represent microfractures in a pre-existing ferroan dolomite grain which allowed fluids to penetrate and replace the core.

Zone selective replacement of dolomite by calcite is observed in Pliocene dolomites from Bonaire. Similar features are observed in some dedolomites (Fritz, 1971; Frank, 1981). In the Trenton, replacement of ferroan dolomite by non-ferroan dolomite could be driven by a number of factors. Ferroan dolomite-ankerite is considered metastable and generally contains excess $CaCO_3$. It is
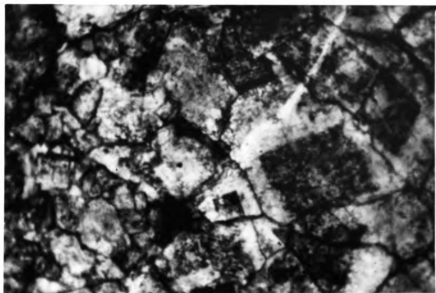
Figure 10a.   Ferroan dolomite cores (stained) with non-ferroan overgrowths. Samples from approximately 120 feet below the cap in the Northville field. Width of field = 0.7 mm.

Figure 10b. Stained thin section showing small Fe-rich zones in non-ferroan dolomite cores. Outer zone is ferroan dolomite. Width of field = 0.35 mm.
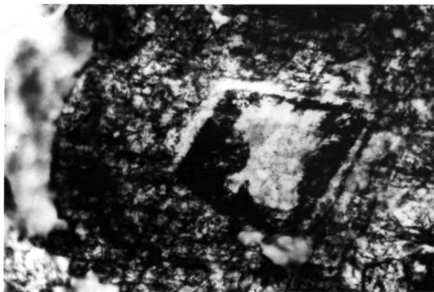
Figure 10c. Irregularly shaped non-ferroan dolomite core. This is evidence of zone selective replacement of ferroan dolomite by non-ferroan fracture dolomite. Width of field = 0.35 mm.

Figure 10d. Ferroan dolomite zone which has been broken by non-ferroan fracture dolomite connecting the core and outer non-ferroan dolomite zone. Width of field = 0.35 mm.

possible that this type of dolomite could be replaced by iron-poor dolomite which may, under certain conditions, have greater stability.

With depth (150-250 feet below the cap) the ferroan cores and ferroan zones disappear and the rock is composed of xenotopic, non-ferroan dolomite with non-ferroan baroque dolomite in voids. This texture is identical to fracture-related dolomites in the Albion-Scipio Field and in other locations throughout the Michigan Basin.

In some samples from the northern part of the basin and the Albion-Scipio trend, ferroan dolomite continues to form after non-ferroan fracture-related dolomite. This is evidenced by thin ferroan overgrowths on rhombic dolomite faces in voids, and in one case larger ferroan overgrowths on non-ferroan dolomite near a stylolite. Although this second ferroan dolomite episode is rarely observed and volumetrically minor, it indicates that Fe^{2+} was being supplied to the system before and after fracture-related dolomite formation. The source of iron for this episode may have been pressure solution of pre-existing ferroan dolomite which formed much earlier.

CHEMISTRY OF DOLOMITE TYPES

The separation of the Trenton dolomites into three major types is based largely on differences in texture and distribution. Major and minor element analyses along with oxygen isotope ratios show important chemical differences between the three types of dolomite. These analyses are presented in Tables 2 and 4 and summarized in Tables 3 and 5.

Major and Minor Element Analyses

A) Cap Dolomite - The Trenton cap dolomites are characterized by the fact that they are rich in iron and would be classified as ferroan dolomite with a

Table 2. Electron microprobe analyses of Trenton dolomites.

Sample		% CaCO$_3$	% MgCO$_3$	% FeCO$_3$	(ppm) Mn	(ppm) Na
Br 3651	Location 1, Figure 1	54.07	42.19	3.74		
	Cap Dolomite	51.47	43.41	5.12		
		52.24	40.95	6.81		
		51.56	43.12	5.32		
		51.59	43.90	4.52		
		52.38	43.62	4.00		
		51.37	42.16	6.47		
		50.34	40.71	8.96		
Br 3656		55.66	35.35	8.99		
		56.06	40.88	3.06		
		55.39	33.90	10.71		
		53.09	39.70	7.21		
		56.26	41.58	2.17		
		54.88	42.82	2.30		
		54.67	42.46	2.87		
		57.38	34.81	7.81		
		52.29	40.06	7.65		
		56.91	36.70	6.39		
		55.70	35.74	8.56		
		54.30	39.16	6.53		
		54.74	41.29	3.97		
		57.41	40.02	2.56		
		56.19	39.32	4.50		
Br 3657		55.71	40.48	3.81	2791	400
		54.72	35.67	9.61		
		55.76	39.49	4.75	2346	459
		55.09	35.95	8.96	4124	562
		52.19	40.21	7.62	4075	355
		54.98	41.99	3.02	1951	281
		57.19	36.59	6.21	3013	289
		56.67	40.52	2.82	1852	378
		55.31	35.20	9.49	4199	540
		53.60	37.63	8.77	2643	430
		54.71	42.52	2.78	1852	229
		55.68	42.07	2.25	2149	214
		55.14	42.09	2.77	1848	226
Br 3660		55.95	34.87	9.18	2522	370
		58.71	33.63	7.67	1701	529
		56.92	36.02	7.07		
		55.24	36.67	8.09	4577	586

Table 2 (continued).

Sample		% CaCO$_3$	% MgCO$_3$	% FeCO$_3$	(ppm) Mn	(ppm) Na
Br 3660	Non-ferroan Overgrowths	54.85	43.58	1.57	1180	311
		56.31	42.67	1.07	1167	474
		56.18	43.73	0.91	1332	384
		55.78	42.99	1.23	1706	363
		54.86	43.96	1.18	1154	390
		54.88	44.16	0.95		
E2 3680	Cap Dolomite	52.81	43.05	4.14		
		51.12	41.39	7.48		
		50.72	41.59	7.70		
		52.30	44.27	3.73		
		50.65	40.41	8.94		
		51.50	44.31	4.19		
		51.84	45.99	2.18		
		51.78	44.60	3.61		
E2 3683		53.91	36.90	9.19		
		57.96	35.70	6.35	4314	273
		53.16	34.30	12.53	4638	273
		55.17	37.88	6.95		
		55.58	36.29	8.13	4350	211
		56.35	33.59	10.06	3775	238
		54.00	35.42	10.57	5141	256
		55.10	42.75	2.15	3637	291
		55.92	34.66	9.42	3703	291
		55.52	32.40	12.08	5609	344
		54.25	36.30	9.46	4207	423
		55.23	34.90	9.87	5788	282
		55.32	41.68	3.00	2876	458
		58.26	33.14	8.60	3128	264
		56.30	38.18	5.52	3739	432
		57.77	33.62	8.61	3452	388
		58.12	34.53	7.35	4782	352
		57.86	33.77	8.37	6292	352
		55.74	33.82	10.45	5824	335
		58.25	34.08	7.68	4134	352
		57.28	32.28	10.44	4494	291
		56.55	40.53	2.92		
		55.20	34.88	9.91	7514	352
		57.02	39.43	3.35	3523	449
		57.25	34.03	8.72	4063	238
		59.47	32.19	8.34	3487	881
		56.92	35.52	7.55	3020	300
		56.72	34.05	9.23	4314	273

Table 2 (continued).

Sample		% CaCO$_3$	% MgCO$_3$	% FeCO$_3$	(ppm) Mn	(ppm) Na
E2 3683	Non-ferroan Overgrowths	55.55	42.85	1.60		
		55.65	43.38	0.98		
		56.71	43.06	0.23		
		56.28	42.14	1.57		
E1 3680B	Zoned Dolomite - non-ferroan and ferroan - Core	54.48	45.46	0.06		
	Overgrowth (1)	52.04	44.52	3.45		
	Overgrowth (2)	55.94	42.65	1.40		
	Core	55.41	43.96	0.63		
		51.59	47.12	1.09		
	Overgrowth	52.70	42.54	4.76		
JF 6101	Location 7, Figure 1	54.05	40.61	5.34	5836	234
		57.32	29.54	13.13		
		55.24	34.37	10.38	5615	437
		56.44	32.56	11.00	5764	709
		56.48	32.06	11.46	3187	395
		56.38	33.48	9.72	3773	457
		53.64	34.28	12.08	3022	
		54.35	34.05	11.60	3194	400
		55.74	32.23	12.02	2746	257
JF 6116		54.97	37.16	7.88		
		53.73	39.61	6.66		
		56.90	37.42	5.67		
		57.93	30.67	11.37		
		55.60	34.42	9.96		
		52.14	41.59	6.27		
		54.45	34.70	10.84		
		55.62	33.58	10.80		
JF 6114		55.79	34.50	9.71	4002	378
		57.08	37.02	5.90	4916	
		56.06	38.95	5.00	4545	367
		57.96	35.58	6.29	4346	244
		56.43	30.15	13.41	2618	
JF 6164		53.43	43.00	3.56		
		54.50	35.90	9.60	2544	280
		53.15	36.34	10.51	4920	125
		55.20	32.81	11.99	4003	284
		57.30	40.27	2.42		
		53.39	40.77	5.65	2049	213

Table 2 (continued).

Sample		% CaCO$_3$	% MgCO$_3$	% FeCO$_3$	(ppm) Mn	(ppm) Na
C-5	Location 2, Figure 1	51.4	44.1	4.5		
	Ferroan Dolomite	50.3	44.4	5.3		
		54.6	40.5	4.9		
		56.9	37.3	5.8		
		54.1	40.6	5.3		
		55.0	38.2	6.7		
		49.0	44.5	6.4		
		55.6	38.8	5.6		
C-2		57.2	36.2	6.6		
		55.6	36.6	7.8		
		54.1	38.8	7.1		
		50.9	47.9	6.2		
		55.6	37.4	7.0		
C-10		52.5	42.1	5.4		
		53.7	40.8	5.5		
22825	Location 13, Figure 1	57.1	34.6	10.5		
	Ferroan Dolomite	54.4	42.8	2.9		
		57.5	32.5	9.9		
		53.7	36.8	9.5		
		57.0	33.1	9.8		
		57.2	29.9	13.0		
		57.9	30.4	11.7		
		57.0	31.8	11.3		
		53.5	38.0	8.5		
		52.4	43.8	3.7		
21795	Location 14, Figure 1	50.4	44.6	5.0		
		52.2	42.6	5.2		
		53.9	39.0	7.2		
		55.3	36.1	8.6		
		53.1	44.4	2.5		

Table 2 (continued).

Sample		% CaCO₃	% MgCO₃	% FeCO₃	(ppm) Mn	(ppm) Na
S 6053	Location 11, Figure 1	50.01	43.40	6.48		
		51.86	40.77	7.37		
		52.31	43.63	4.06		
		54.04	42.08	3.88		
		54.42	41.68	3.91		
		49.52	47.19	3.29		
S 6053	Non-ferroan Overgrowths	52.29	47.50	0.20		
		49.95	49.79	0.25		
		49.82	49.11	1.08		
		51.17	47.89	0.94		
		51.28	48.38	0.13		
		52.51	47.40	0.09		
S 6084	Ferroan Dolomite	55.90	40.25	3.86	1548	416
		55.38	40.69	3.93		
	Non-ferroan Overgrowths	57.66	41.87	0.47	1169	314
		54.11	45.58	0.30	1056	464
		54.91	43.99	1.10		
		55.62	43.69	0.69	1097	374
S 7773	Location 10, Figure 1	50.34	43.68	5.94		
	Ferroan Dolomite	52.79	40.43	6.78		
		51.15	41.60	7.25		
		50.96	40.72	8.31		
		53.25	43.68	3.07		
		51.17	45.26	3.57		
		53.36	40.87	5.77		
	Non-ferroan Overgrowths	54.05	44.98	0.97		
		54.27	45.67	0.06		
		52.08	47.27	0.65		
S 7815	Ferroan Dolomite	56.80	42.53	2.52	2007	447
		50.96	45.94	3.10	1494	423
		52.21	39.40	8.39	1195	484
		54.22	42.89	2.89	1471	349
		53.83	37.49	8.68		
S7813	(Complex Zoned Dolomite) Ferroan Dolomite (Core)	53.11	44.56	2.34		
	Overgrowth	52.64	39.02	8.34		
	Core	53.59	44.19	2.22		
	Overgrowth	51.77	41.83	6.41		
		51.79	38.55	9.65		

Table 2 (continued).

Sample		% CaCO$_3$	% MgCO$_3$	% FeCO$_3$	(ppm) Mn	(ppm) Na
S-7813	Core	52.91	44.88	2.21		
		52.87	45.72	1.41		
	Overgrowth	52.63	39.02	8.35		
S 7774	(Complex Zoning)	55.48	37.83	6.69		
		59.30	36.64	4.07		
	Core	56.46	42.23	1.22		
	Overgrowth	55.52	44.05	0.43		
	Core	54.94	43.94	1.12		
	Overgrowth	55.40	42.84	1.76		
	Core	55.73	43.71	0.56		
	Overgrowth	54.55	36.37	9.09		
	Core	56.27	38.98	4.75		
	Overgrowth	59.03	40.17	0.80		
ST 9904/ 5-5C	Location 9, Figure 1	55.90	35.47	8.63	4401	269
	Basin Center	54.24	35.84	9.92	5769	551
		51.56	35.93	12.51	6950	360
		50.50	36.38	13.12	7758	435
		53.09	35.66	11.25	6169	360
		55.84	34.01	10.15	4983	415
ST 9904- 6A		55.65	32.46	11.89	4519	495
		54.69	32.95	12.37	3015	438
		56.50	36.43	7.07	5755	530
		59.84	33.87	6.29	5787	543
		57.55	36.29	6.16	6304	352
		58.75	35.72	5.54	5251	367
		57.79	36.24	5.96	6233	515
DT 9926A	Location 9, Figure 1	55.21	38.88	5.91		
	Basin Center	51.73	45.11	3.16		
		55.52	37.80	6.69		
DT 9926B		52.09	42.35	5.56		
		56.85	34.83	8.32		
D 3 6	Albion Scipio - Fracture	56.50	43.45	0.05		
	Dolomite	55.57	44.35	0.08		
		56.08	43.84	0.07		
		51.83	48.12	0.05		
		52.29	47.67	0.04		
		53.30	46.60	0.09		

Table 2 (continued).

Sample		% CaCO$_3$	% MgCO$_3$	% FeCO$_3$	(ppm) Mn	(ppm) Na
D 3 6	Albion Scipio - Fracture Dolomite	50.43 53.50	49.50 46.42	0.07 0.08		
D1 4 6		55.19 50.25 51.17 53.95	44.71 49.27 48.60 46.01	0.09 0.48 0.22 0.04		
D 23		49.63 51.90 53.03	49.45 47.49 45.52	0.92 0.62 1.45		
K 8		54.37 54.99 55.19 54.88 56.13	45.09 43.81 44.43 44.03 43.24	0.54 1.20 0.38 1.08 0.63	1468 1491 1182 1258	407 233 109 184
D 4 6		50.99 53.91 51.01	48.69 45.60 48.18	0.32 0.55 0.09	2049 1632 1625	538 333 312
F 4		54.02 53.89 51.27 52.85 53.08	45.92 45.56 48.21 46.40 46.45	0.06 0.55 0.52 0.78 0.47	1305 1528 1750 1539	338 343 358 329
W2 3063	Location 3, Figure 1 Fracture Dolomite	52.26 51.12 52.83 52.07 53.00 53.25	47.51 48.81 45.49 47.88 45.06 46.40	0.23 0.07 1.69 0.05 1.93 0.35	1540 1306 285 1047	450 244 331 278
W2 3070		51.34 52.79 52.97 52.31 50.79	48.51 47.13 46.97 47.60 49.09	0.15 0.08 0.06 0.09 0.11		
W2 3198		54.13 50.43 51.95 52.70	45.82 49.50 47.99 47.23	0.05 0.07 0.06 0.07	583 722 729 994	229 215 326 355

Table 2 (continued).

Sample		% CaCO$_3$	% MgCO$_3$	% FeCO$_3$	(ppm) Mn	(ppm) Na
W2 3087	Location 3, Figure 1	50.65	49.31	0.08	2517	344
	Fracture Dolomite	49.69	50.22	0.08		
		51.00	48.95	0.05	2193	485
		50.47	49.47	0.06	2085	379
		51.34	48.59	0.07	1802	511
		50.46	48.71	0.84	1798	388
W2 3065		52.55	47.23	0.21	1581	570
		53.30	45.48	1.22	2734	319
		53.26	46.68	0.06		
		53.93	44.96	1.11	1791	162
W2 3094A		50.29	49.65	0.07		
		50.34	49.57	0.09		
		50.15	49.77	0.08		
		51.00	48.94	0.06		
		50.58	49.31	0.10		
W2 3092		50.54	49.37	0.09		
		51.74	48.20	0.06		
		50.66	49.28	0.06		
S 6117	Location 11, Figure 1	54.01	45.86	0.13		
	Fracture Dolomite	52.58	46.25	1.17		
		56.16	43.73	0.11		
		57.41	42.38	0.20		
		54.82	45.10	0.08		
		53.82	46.09	0.09		
		53.26	45.28	1.46		
S 8018	Location 10, Figure 1	52.41	47.07	0.29		
		53.38	46.47	0.15		
		55.84	43.43	0.72		
S 7868		52.66	46.58	0.76		
		57.13	42.28	0.59		
		55.87	43.07	1.06		
		55.40	43.86	0.74		
		56.10	43.83	0.07		
		54.06	45.34	0.60		
L124947	Location 12, Figure 1	51.39	48.51	0.10		
	Regional Dolomite	51.39	48.28	0.34		
		50.02	49.92	0.06		
		50.42	49.50	0.08	1381	307

Table 2 (continued).

Sample		% CaCO$_3$	% MgCO$_3$	% FeCO$_3$	(ppm) Mn	(ppm) Na
L124947	Location 12, Figure 1	50.45	49.95	0.09		
	Regional Dolomite	50.60	49.31	0.09	1587	267
		50.67	49.26	0.07		
		50.63	49.30	0.07		
L124948		50.03	49.88	0.09	974	364
		50.39	49.53	0.08	953	421
		50.89	49.01	0.10	936	612
		49.73	50.18	0.09	806	567
		49.02	50.89	0.09	709	564
L124979		50.15	49.75	0.09	722	335
		50.04	49.89	0.07	751	341
		50.24	49.68	0.08	671	470

Estimated errors of microprobe analyses as % of reported value: CaCO$_3$ ≃ ±5%; MgCo$_3$ ≃ ±3%; FeCO$_3$ ≃ ±5%; Mn ≃ ±16%; Na ≃ ±35%.

Table 3. Mean values for major and minor element analyses of Trenton dolomites.

	FeCO$_3$%		Mn (ppm)		Na (ppm)	
	$\bar{x}$	s	$\bar{x}$	s	$\bar{x}$	s
Cap Dolomites	7.2[1] n = 115	3.0	3830[1] n = 58	1267	341[1,3] n = 60	123
Basin Center	8.3[2] n = 19	2.9	5261[2] n = 16	1357	411[3,4] n = 16	98
Fracture Dolomites	0.4[1,2] n = 77	0.4	1477[1,2] n = 33	520	333[2,4] n = 28	111
Regional Dolomites	0.1[1,2] n = 16	0.1	949[1,2] n = 10	305	425[1,2] n = 10	122

Superscripted numbers indicate the results of T-tests. Population means carrying the same superscript are significantly different at α = 0.05.

Table 4. $\delta^{18}O$ and $\delta^{13}C$ analyses of Trenton dolomites and calcites.

Sample	Location-Figure 1	Lithology	$\delta^{18}O_{PDB}$	$\delta^{13}C_{PDB}$
Br-3653	1	Cap Dolomite	-6.7°/oo	-0.4°/oo
Br-3653a			-7.7	-0.7
Br-3654			-7.6	-0.4
Br-3657			-8.4	-0.8
E1-3651			-8.0	-0.5
E1-3652			-7.2	-1.2
E1-3658			-7.6	-0.4
E1-3655			-7.6	-0.9
E1-3654			-7.8	-1.7
E1-3656			-7.8	-0.9
22790	13		-7.0	-0.2
ST-9904/5-2B	9	Basin Center (Fe-dolomite)	-8.3	+0.7
ST-9904/5-3B			-8.1	+0.4
ST-2B			-7.7	+1.1
ST-9904B			-7.8	+0.9
DT-9926A			-7.8	-0.9
DT-9934		Baroque (Fe-dolomite)	-9.9	-0.2
D23B	6 Albion-Scipio Field	Fracture Dolomite	-8.6	+0.5
D1-4-M			-7.4	+0.5
D2-23-1			-8.4	+0.6
D3-3-6			-7.8	+0.5
D1-4-6A			-9.4	-0.2
K7B	4		-8.2	-0.1
K6-M			-6.5	+0.5
K10A-M			-9.1	+0.1

42

Table 4 (continued).

Sample	Location–Figure 1	Lithology	$\delta^{18}O_{PDB}$	$\delta^{13}C_{PDB}$
K10A-V	4 Albion-Scipio Field	Fracture Dolomite (Baroque)	-9.3°/oo	0.0°/oo
K3-M		Fracture Dolomite	-9.1	-0.9
K3-V		Fracture Dolomite (Baroque)	-8.8	-0.1
K4		Fracture Dolomite	-6.9	-0.4
HK*			-9.1	
			-9.7	
			-8.2	
			-8.8	
AGM*			-9.1	
CR*			-8.2	
H-K-K*			-8.1	
Br-3791A	1 Northville Field	Fracture Dolomite (Baroque)	-11.2	+0.2
Br-3802A		Fracture Dolomite	-7.9	+0.3
Br-3802B			-7.3	-0.1
Br-3782			-8.1	-0.7
Br-3820			-8.5	+0.3
Br-3841			-8.0	+0.4
T-N*			-7.4	
			-8.6	
			-9.0	
			-9.0	
			-9.0	
			-9.2	
W2-3198	3	Fracture Dolomite (Baroque)	-9.5	0.0
W2-3187		Fracture Dolomite	-9.8	+0.2
W2-3171			-9.2	+0.2
W2-3211			-10.1	+0.5

Table 4 (continued).

Sample	Location-Figure 1	Lithology	$\delta^{18}O_{PDB}$	$\delta^{13}C_{PDB}$
			$-10.8\,^o/oo$	$0.0\,^o/oo$
W2-3218	3	Fracture Dolomite	-10.8	0.0
W2-3177	12		-10.5	+0.1
L12-5185			-9.2	-1.1
L12-5173A			-10.8	+0.5
L12-5201D			-11.2	-0.2
L12-5201E			-11.3	-0.7
L12-5201F			-11.4	-0.7
S6082	11		-8.5	-0.8
S6101			-8.0	-1.6
S6117.1			-7.8	+0.9
S7813.6	10		-8.3	+0.6
S7815.8			-9.4	+0.3
S7817			-8.7	+0.6
S7837			-8.6	+1.5
S7755A			-8.8	-0.8
S7755B			-8.4	-0.9
S8018			-13.4	-1.2
S8011			-9.1	-0.5
L12-4970	12	Regional Dolomite	-7.4	-0.6
L12-4970A			-7.3	-0.5
L12-4948			-6.2	-0.4
L12-4984			-5.6	0.0
L12-5086			-7.6	+0.3
EW1*	Eastern Wisconsin		-6.5	
EW2*			-6.0	
EW3*			-6.8	
EW4*			-7.8	

Table 4 (continued).

Sample	Location-Figure 1	Lithology	$\delta^{18}O_{PDB}$	$\delta^{13}C_{PDB}$
EW5*	Eastern Wisconsin	Regional Dolomite	-5.6°/oo	+0.4°/oo
E2-3992	1	Brachiopod (LM Calcite)	-5.2	+0.5
E-9			-5.4	-0.5
W2-3065	3		-5.1	+0.5
S6027.9	11		-5.6	-0.2
S7731.6	10	Micrite (Calcite)	-4.5	-0.4
E1-3665	1		-5.1	+0.7
L12-5106	12	Vein Calcite	-5.5	+0.4
DT-9923B	9		-6.4	

*Data from R. M. Lloyd, personal communication.

Approximate error of analysis ≈ 0.1°/oo.

Table 5. Mean values for oxygen and carbon isotopes of Trenton dolomites and calcites.

	$\delta^{18}O_{PDB}$		$\delta^{13}C_{PDB}$	
	$\bar{x}$	s	$\bar{x}$	s
Cap Dolomites	-7.7°/oo[1] n = 13	0.5	-0.7°/oo n = 13	0.7
Basin Center	-7.9°/oo[2] n = 5	0.3	+0.8°/oo n = 5	0.3
Fracture Dolomites	-9.0°/oo[1,2,3] n = 51	1.3	0.0°/oo n = 32	0.6
Regional Dolomites	-6.8°/oo[3] n = 5	0.9	-0.2°/oo n = 5	0.4
Eastern Wisconsin	-6.5°/oo n = 5	0.8		

Superscripted numbers indicate results of T-tests. Population means carrying the same superscript are significantly different at α = 0.05.

few analyses falling in the ankerite range (Figure 11). Analyses range from 2.15 to 13.41 mol% $FeCO_3$ ($\bar{x}$ = 7.2 mol% $FeCO_3$). The cores of cap dolomites are generally more iron-rich than the outer portion of the grains. However, no regular decrease in $FeCO_3$ content is observed from crystal center to edge, i.e., % $FeCO_3$ does not appear to vary in a predictable manner. The cap dolomites are also relatively rich in Mn ($\bar{x}$ = 3830 ppm) and contain relatively low levels of Na ($\bar{x}$ = 341 ppm).

The tendency of ferroan dolomite-ankerite to contain excess $CaCO_3$ has been recognized in a number of studies (Goldsmith and Graf, 1958, 1960; Goldsmith, et al., 1961; Shaw, 1959; Rosenberg, 1967; Murata, et al., 1972; Rosenberg and Foit, 1979; Irwin, 1980; M'Rabet, 1981). Rosenberg and Foit (1979) suggest that the addition of excess $CaCO_3$ would serve to reduce the effects of octahedral distortions produced by the substitution of Fe^{2+} for Mg^{2+}.

Ferroan dolomites from the Trenton also contain excess $CaCO_3$ as seen in Figure 12. The scatter of data points in Figure 12 indicates that there is no systematic, predictable variation in the amount of excess $CaCO_3$ with increasing $FeCO_3$ content. This is also reflected in the X-ray diffraction patterns of the cap dolomites which show poorly developed ordering reflections. This indicates that there is no regular distribution of Ca, Mg, and Fe within the crystal.

B) Regional Dolomite - Regional dolomite from the extreme western edge of the Michigan Basin is chemically distinct from the other Trenton dolomites. The regional dolomites are non-ferroan (0.04-0.34 mol% $FeCO_3$, $\bar{x}$ = 0.10%), contain relatively low levels of Mn ($\bar{x}$ = 949 ppm), and low levels of Na ($\bar{x}$ = 425 ppm). The regional dolomites have well-developed ordering reflections and nearly stoichiometric proportions of Ca and Mg (Figure 12).

C) Fracture-Related Dolomite - The fracture dolomites are non-ferroan and generally Ca-rich. $FeCO_3$ contents range from 0.03 to 2.3% with a mean
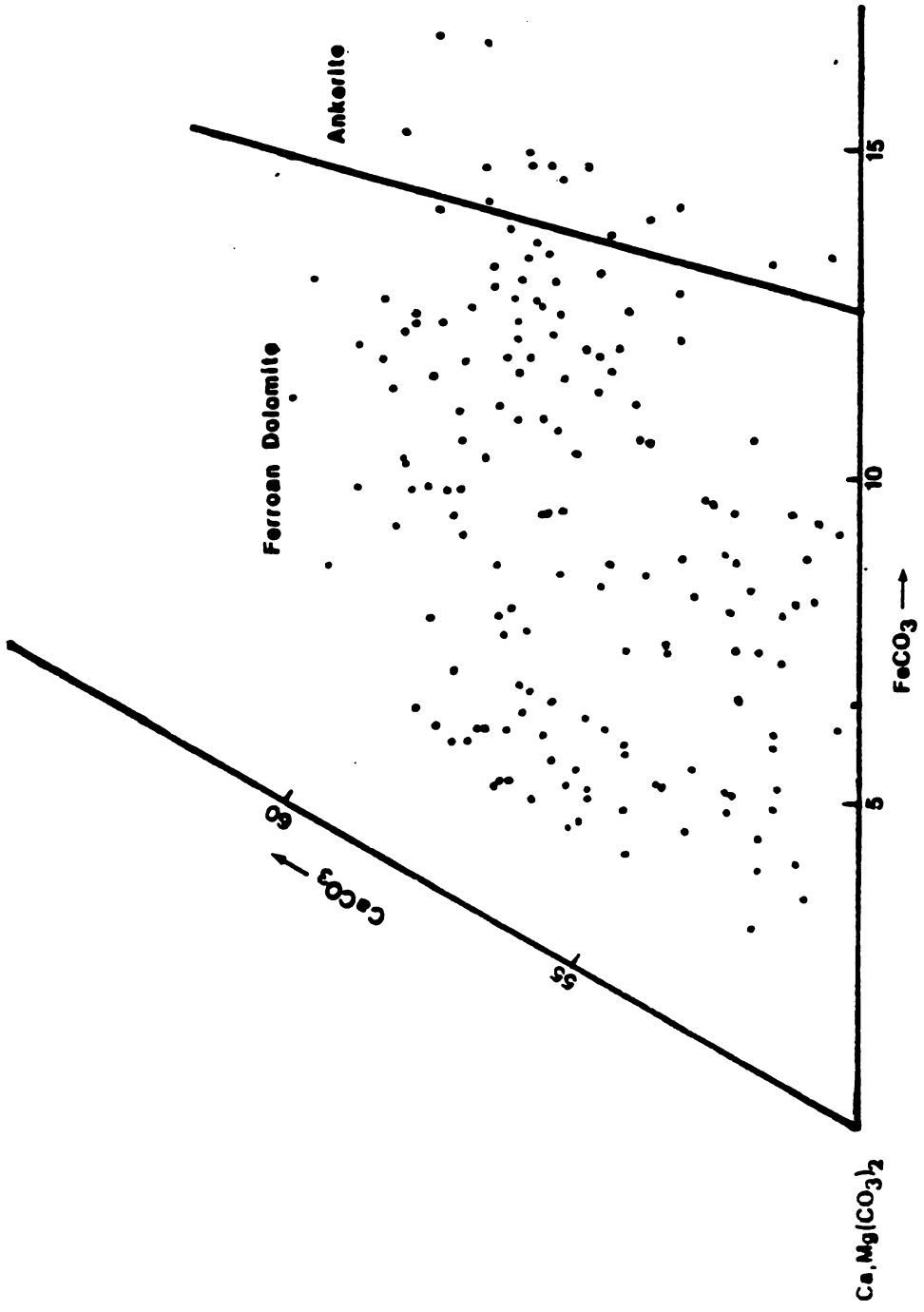
Figure 11. Composition of ferroan dolomites from the Trenton Formation.
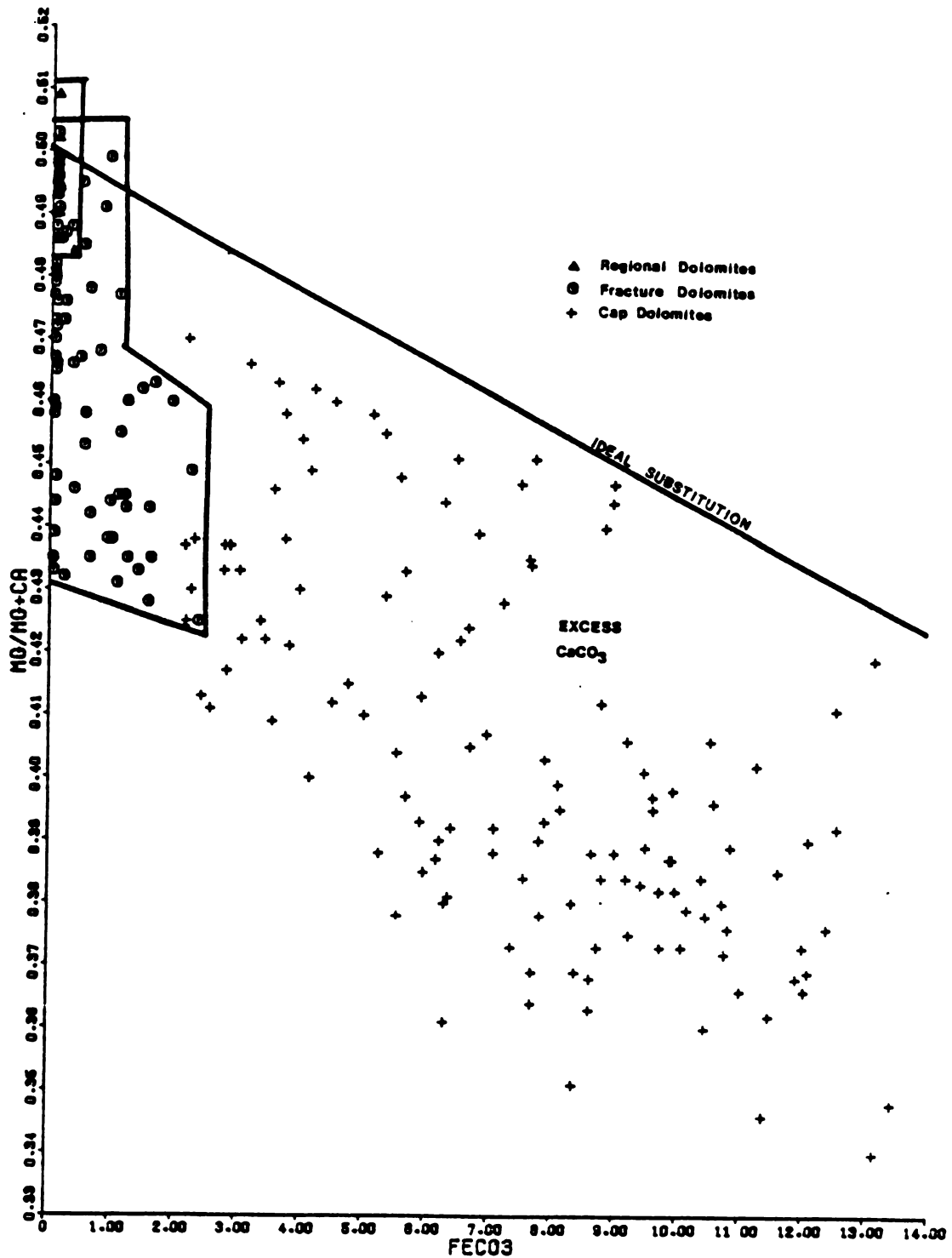
Figure 12. Mg/Mg+Ca vs. FeCO$_3$ mol% for Trenton dolomites. Ideal substitution line represents 1 for 1 substitution of Fe^{2+} for Mg^{2+} in dolomite. Nearness to this line is a measure of dolomite stoichiometry.

value of 0.40 mol% $FeCO_3$. The fracture-related dolomites have intermediate levels of Mn ($\bar{x}$ = 1477 ppm) and low levels of Na ($\bar{x}$ = 333 ppm). In contrast to regional dolomites, fracture-related dolomites range from essentially stoichiometric Ca/Mg ratios to as high as 8 mol% excess $CaCO_3$ (Figure 12). In contrast to the ferroan cap dolomites, the fracture-related dolomites have well-developed ordering reflections indicating a regular arrangement of Ca and Mg octahedra.

Oxygen and Carbon Isotope Analyses

$\delta^{18}O$ and $\delta^{13}C$ values for Trenton dolomites and limestones are presented in Table 4 and summarized in Table 5. $\delta^{13}C_{PDB}$ values for the three types of dolomite are similar and generally range between $-1^{\circ}/oo$ and $+1^{\circ}/oo$. Oxygen isotope ratios are different for each dolomite type.

The mean $\delta^{18}O_{PDB}$ value for regional dolomite is $-6.8^{\circ}/oo$. This value is similar to a mean $\delta^{18}O_{PDB}$ value of $-6.5^{\circ}/oo$ for Mid-Ordovician dolomites from Eastern Wisconsin (Table 5). The cap dolomites have a mean $\delta^{18}O_{PDB}$ value of $-7.7^{\circ}/oo$. Fracture-related dolomites have very depleted ratios with a mean $\delta^{18}O_{PDB}$ of $-9.0^{\circ}/oo$. Baroque, void filling dolomites found in the Albion-Scipio Field have $\delta^{18}O_{PDB}$ values ranging from $-8.8^{\circ}/oo$ to $-11.2^{\circ}/oo$ with a mean of $-9.8^{\circ}/oo$.

The usefulness of oxygen isotope analyses in the study of dolomite has been severely limited by our inability to precipitate dolomite at low-temperatures in the laboratory (see Carpenter, 1980; Land, 1980). The degree of equilibrium fractionation of oxygen isotopes between dolomite-water and dolomite-calcite at low temperature is therefore uncertain. Estimates of these fractionation factors are obtained by extrapolating from high temperature synthesis studies (Northrup and Clayton, 1966; O'Neil, et al., 1969; Matthews and Katz, 1977). Complicating the situation, the possibility exists that when dealing with ancient dolomites the

$\delta^{18}O$ ratios of these rocks are not those obtained during dolomitization but have been altered to varying degrees during burial and neomorphism (see Land, 1980). For these reasons, interpretation of oxygen isotope ratios of dolomites must be tempered with some caution.

The fact that the Trenton regional, cap, and fracture dolomites each have distinctly different $\delta^{18}O$ signatures is further evidence that they have different origins. Petrographic relations have shown that the dolomites formed in the order: 1) regional, 2) cap, 3) fracture. $\delta^{18}O$ values also become progressively more depleted in this order. Such a trend could be explained by dolomitization or recrystallization at progressively higher temperatures. Detailed discussion of $\delta^{18}O$ ratios for each of the three dolomite types appears in the sections on their origins.

Isotopic Composition of Ordovician Seawater

It has been noted that carbonate rocks show a general trend of more depleted $\delta^{18}O$ ratios with increasing geologic age (Clayton and Degens, 1959; Degens and Epstein, 1962; Fritz, 1971; Perry and Tan, 1972; Veizer and Hoefs, 1976; Brand and Veizer, 1981; Brand, 1982). Veizer and Hoefs (1976) evaluated secular trends in oxygen isotope ratios of carbonate rocks with ages from 100-2800 m.y. These trends may be the result of variations in the oxygen isotope composition of ancient oceans (Fritz, 1971; Perry and Tan, 1972; Veizer, 1977; Dickson and Coleman, 1980; Brand and Veizer, 1981; Brand, 1982).

Brand and Veizer (1981) estimate that Silurian seawater was depleted in $\delta^{18}O$ by approximately 5.5°/oo and Mississippian seawater depleted by about 1.5°/oo when compared to Recent seawater. Brand (1982) suggests that Carboniferous seawater had $\delta^{18}O_{SMOW}$ about 1.2°/oo lighter than Recent seawater.

Brand (1982) advocates the use of relatively unaltered ancient brachiopods to estimate the isotopic composition of ancient seawater. Articulate brachiopods are thought to precipitate low-Mg calcite in isotopic equilibrium with seawater (Lowenstam, 1961). Four brachiopods from limestone portions of the Trenton were selected for isotope analysis. Each brachiopod exhibited a well-preserved, wavy, fibrous two-layer shell structure and was composed of low-Mg calcite. Each sample was obtained from a different part of the basin as to avoid sampling local variation. If the assumption is made that these brachiopods are largely unaltered, they can be used to estimate the isotopic composition of Ordovician seawater of the Michigan Basin. Figure 13 shows the isotopic range of the brachiopod samples ($\delta^{18}O_{PDB}$ = -5.1°/oo - -5.6°/oo; $\delta^{13}C_{PDB}$ = +0.5°/oo - -0.5°/oo. Three analyses of micrite are also plotted.

The variation of $\delta^{13}C$ values is well within the limits for marine carbonates. The small variation of $\delta^{18}O$ for the brachiopods indicates that they formed from water of the same isotopic composition. These brachiopods may have formed from Ordovician seawater in the Michigan Basin which had an oxygen isotope ratio of approximately -5°/oo$_{SMOW}$. Micrite samples have $\delta^{18}O$ values very near brachiopods and probably stabilized early in diagenesis under the influence of ambient seawater. This estimate of Ordovician seawater is consistent with the results of Veizer and Hoefs (1976) study of secular trends in marine carbonates.

DISCUSSION

The chemical and textural characteristics and the distribution of these dolomite types are strong evidence that they formed under differing conditions and probably in different diagenetic environments. The chemical characteristics and distribution of each of the three dolomite types can be used to set basic

Figure 13. $\delta^{18}O$ vs $\delta^{13}C$ for selected Trenton calcites.

constraints on models for their origin. Although this study is primarily concerned with determining the origin of the cap dolomite some inferences about the origin of the other dolomite types can be made.

Regional Dolomite

The Trenton regional dolomite is volumetrically more important than either the cap or fracture dolomites. In order to form such a thick, laterally continuous sequence of dolomite many pore volumes of dolomitizing solutions must pass through a limestone (Land, 1980). This is best accomplished near the surface or at shallow levels of burial where sediment permeability and flow rates are high.

The regional dolomites along the western edge of the Michigan Basin may be correlative with Middle Ordovician dolomites of the Galena Group in eastern Wisconsin. Dolomites of eastern Wisconsin and western Michigan have nearly identical $\delta^{18}O$ values (Table 4) and are considered time-stratigraphic equivalents. Badiozamani (1973) proposed a mixed-water origin for Ordovician dolomites of Wisconsin. Although a mixed-water origin for these dolomites is not advocated here, it is suggested that the Trenton regional dolomites formed at or near the earth's surface during early diagenesis.

Regional dolomites are depleted in $\delta^{18}O$ by approximately 1-2°/oo when compared with Trenton limestones (Table 4). The equilibrium $\Delta^{18}O_{D-C}$ at 25°C is unknown at this time but the best estimate appears to be near +3°/oo (Land, 1980). Thus, dolomite which forms in equilibrium with calcite in an open system would be expected to have $\delta^{18}O$ values approximately 3°/oo heavier than co-precipitated calcite. Strict application of such an equilibrium fractionation factor to dolomite and calcite which clearly did not co-precipitate is erroneous. However, it has been suggested elsewhere that slow dolomitization of a fine-grained limestone via grain boundary diffusion in a rock dominated system may

approximate equilibrium and with time result in dolomites with $\delta^{18}O$ more positive than the precursor limestone (Mattes and Mountjoy, 1980; McKenzie, 1981).

In order to explain the depleted $\delta^{18}O$ values of the regional dolomites one of the following must have occurred: a) Dolomitization took place at low temperature with the involvement of large amounts of meteoric water such that the total oxygen source (rock + water) was 2°/oo or more depleted in $\delta^{18}O$ when compared to the estimated oxygen isotope composition of Ordovician seawater. Dolomitization in the mixing zone could conceivably supply such an oxygen source. b) The regional dolomites formed at low temperature, near the earth's surface as a disordered dolomite phase and later recyrstallized at depth, acquiring a more depleted $\delta^{18}O$ ratio by interaction with pore waters at elevated temperatures (Land, 1980). Mid-Ordovician dolomites from western Wisconsin have more positive $\delta^{18}O$ values ($\delta^{18}O_{PDB} \simeq -4°/oo$) than regional dolomites of the Michigan Basin (Badiozamani, 1973; Gregg, 1982). This may be the result of recrystallization of the regional dolomites of western Michigan at a time in the past when they were more deeply buried.

If the present oxygen isotope ratios of the regional dolomites are largely primary (i.e., acquired at low T from seawater or mixed-waters) and our estimate of Ordovician seawater in the Michigan Basin approximately correct, an evaporative model for dolomitization is inconsistent with the $\delta^{18}O$ data. Evaporation of seawater produces solutions with more positive $\delta^{18}O$ ratios than seawater (Lloyd, 1966). Dolomite precipitated from such a solution would have more positive $\delta^{18}O$ ratios than nearby marine limestones.

Fracture-Related Dolomite

The distribution of the fracture dolomite, along large and small scale fractures, faults, and veins requires that dolomitization occurred after

lithification of the Trenton. The exact timing of dolomitization has not been demonstrated, however in the Albion-Scipio field, Shaw (1975) suggests that it occurred sometime after Niagaran (Silurian) time.

Post-lithification, epigenetic dolomites described by Mattes and Mountjoy (1981) and Choquette (1971) have textural characteristics which are similar to the Trenton fracture dolomites. As pointed out in a previous section, abundant baroque or saddle dolomite is associated with fracture dolomites in the Trenton. Radke and Mathis (1981) have shown that saddle dolomite may be the result of dolomite formation at elevated temperatures. Fluid inclusion work by Shaw (1975) lends support to this and gives a minimum temperature of $80^{\circ}C$ for Albion-Scipio baroque dolomites.

Trenton fracture dolomites have the most depleted $\delta^{18}O$ values determined in this study (Tables 4 and 5) which may be the result of dolomitization at elevated temperature. Vein and void filling baroque dolomites have a mean $\delta^{18}O_{PDB}$ of $-9.8^{\circ}/oo$. Because these dolomites formed by direct precipitation from solution rather than by replacement of pre-existing calcite they provide the best estimate of equilibrium dolomite-water isotopic fractionation. The only available analysis of a water sample from the Albion-Scipio dolomites has a $\delta^{18}O_{SMOW}$ of $-1.4^{\circ}/oo$ (Clayton, et al., 1966). Precipitation of void filling baroque dolomite ($\delta^{18}O_{PDB} = -8.8^{\circ}/oo$ to $-11.2^{\circ}/oo$) from a water with this isotopic composition requires that precipitation occurred at temperatures of approximately $71^{\circ}-89^{\circ}C$ (equation from Matthews and Katz, 1977).

It is likely that the water sample from the Albion-Scipio dolomites used in the above temperature calculation has undergone chemical alteration through time. At present bottom hole temperatures, the baroque dolomites are not in isotopic equilibrium with this water. It is not known whether or not this water is representative of the fracture dolomite forming solutions. The above

temperature calculation is only an estimate based on the limited data available. However, it is interesting to note the close agreement of the temperature estimates obtained from fluid inclusions and oxygen isotopes.

Origin of the Cap Dolomite

As outlined in a previous section, the Trenton cap dolomite unit occurs at the southern and northern edges of the Michigan Basin and is confined to the upper portion of the Trenton at or near the contact with the overlying Utica Shale. The cap dolomite is characterized by the fact that it is unusually rich in iron and manganese. With the possible exception of the extreme western part of the basin, some ferroan dolomite occurs in the upper Trenton throughout the basin. However, only at the periphery of the basin does ferroan dolomite form a distinct, approximately 100% dolomite cap rock unit. Any model for the origin of the cap dolomite must explain both its iron-rich nature and distribution.

In the southern part of the Michigan Basin, the contact between the Trenton and Utica Shale is extremely sharp. This has led to the proposal of an unconformity at the Trenton-Utica contact (Rooney, 1966). Whether or not the Trenton was subaerially exposed prior to the deposition of the Utica Shale is uncertain. Evidence of exposure such as caliche zones and solution features were not observed in this study. Such evidence may have been destroyed during formation of the cap dolomite. In the basin center (where no cap dolomite is present) the Trenton-Utica contact is gradational and consists of approximately 30 feet of interbedded argillaceous limestone (containing ferroan dolomite) and black shale. Because ferroan dolomite occurs throughout most of the basin its existence is not related to the type of contact observed. However, a relationship exists between the abundance of ferroan dolomite (i.e., occurrence of a cap dolomite) and areas where the Trenton-Utica contact is sharp.

The absence of a cap dolomite unit in the basin center cannot be attributed to limits in the amount of Fe^{2+} available during diagenesis. Iron-bearing minerals observed in the dolomitic limestone in the basin center are ferroan dolomite and abundant iron sulfides (identified as pyrite and iron monosulfide with the microprobe). The cap dolomite is made up of ferroan dolomite with trace amounts of iron sulfides (mostly iron monosulfide, rare pyrite). Whole rock iron analyses of samples of Utica Shale and Trenton limestones and dolomites are presented in Table 6. Comparison of analyses of samples from the basin center (ST; Figure 1, Location 9) and cap region (E1, E2, Br1; Figure 1, Location 1) clearly shows that iron availability did not control the distribution of the cap dolomite. In fact, in the basin center the upper 0.5-1.0 foot of the Trenton is 2-3% richer in Fe_2O_3 than the cap dolomite. The difference seen between basin center and edge is clearly a function of mineralogy rather than iron content.

Sources of Iron. There are two possible sources of iron which could explain the abundance of ferroan dolomite and/or iron sulfides in the upper portion of the Trenton: 1) Fe^{2+} is transferred to the upper Trenton from the Utica Shale during dewatering and diagenesis of the shale. 2) The pre-existing limestone of the upper Trenton was originally rich in iron (detrital Fe-oxides, clays, organics) and was its own source of iron during dolomitization.

The Utica Shale as a source of iron for the upper Trenton is supported by the following lines of reasoning: a) The fact that throughout most of the basin, ferroan dolomite is present and iron concentrations are high in the upper part of the Trenton requires a basin-wide source of iron. The Utica Shale is iron-rich (Table 6) and continuous throughout the basin. b) Much of the iron transported in the aqueous environment is present as thin iron-oxide coatings adsorbed on detrital mineral grains (Carroll, 1958; Berner, 1970, 1971). Such iron oxide coatings have a tendency to form on clay minerals and are therefore abundant in

Table 6. Whole rock iron analyses (%Fe$_2$O$_3$) of Trenton
dolomites and limestones and the Utica Shale.

Sample	Lithology	Depth Below Utica-Trenton Contact (ft.)	%Fe$_2$O$_3$
E1-3651 (loc. 1)	Ferroan cap dolomite	1	4.33
E1-3653		3	3.55
Br-3653		3	3.57
E2-3680		4	4.29
Br-3654		4	3.77
E2-3685		9	4.29
E1-3665	Limestone w/ ferroan dolomite	15	1.60
E2-3707		31	1.11
Br-3746	Limestone	94	0.45
E2-3808		132	0.37
E2-3896		220	0.32
E2-3951		275	0.27
ST-9904B (loc. 9)	Fe-dolomite, Fe-sulfides, Calcite	1	7.56
ST-9904-7A		1	6.41
ST-9904/5-4A		0.5	8.97
ST-9904/5-3B		0.5	5.65
ST-9906	Limestone w/ Fe-dolomite and Fe-sulfides	2	1.27
ST-9911		7	2.51
ST-9916		12	0.90
ST-9921		17	1.37
ST-9884	Utica Shale		6.76
ST-9892			6.19
ST-9896			7.95
ST-9903/5			7.30
JF-6101/5 (loc. 7)	Limestone w/ Ferroan dolomite	0.5	1.44
JF-6108		7	1.10
JF-6116		15	1.17
JF-6148		47	0.58
JF-6156		55	0.77
JF-6179		78	0.94
W2-3065 (loc. 3)		32	1.20
W2-3084		51	0.97
W2-3087		54	1.02
L12-4947 (loc. 12)		1	0.99
L12-4948		2	2.07
L12-4950		4	2.98
L12-5092		146	0.94
L12-5163		217	0.32

fine-grained sediments. Under reducing conditions (established soon after burial), Fe^{2+} may be released by reduction of unstable iron-oxide coatings (Carroll, 1958; Curtis, 1967). Iron may also be reduced within the clay lattice and released via ion-exchange processes (Drever, 1971; Heller-Kallai and Rozenson, 1978; Irwin, 1980). Iron bound with organic matter (humic material) may be released during bacterial oxidation. In organic-rich sediments such as the Utica Shale and Trenton, this source of iron may be substantial. c) During compaction and dewatering of shales most of the fluids are expelled upward and toward the edges of a subsiding basin (Margara, 1974; Burst, 1969). To a limited extent, lateral and downward expulsion can occur from less permeable beds (shales) to more permeable beds (sands and limestones). In the case considered here, it is possible for fluids to be transferred from the Utica Shale to the upper Trenton during burial and compaction. d) If the Utica Shale acted as a source for iron enrichment in the upper Trenton the whole rock iron content would be expected to decrease with distance from the source. Such is the case in both the basin center and the cap region (Table 6).

The above may be considered important sources of iron relatively early in diagenesis of the Utica Shale. At greater depths and higher temperatures the transformation of smectite clay layers into smectite/illite can also release Fe^{2+} (Burst, 1969; Perry and Hower, 1972; Hower, et al., 1976; Boles, 1978; Boles and Franks, 1979). Petrographic evidence indicates that some ferroan dolomite in the Trenton cap (albeit a relatively small amount) formed after lithification and the onset of pressure solution. Clay mineral transformation may have been the source of iron for the late stages of ferroan dolomite. Today the Utica and Trenton are buried only 3000-6000 feet in the cap region. Although somewhat tenuous, stratigraphic reconstructions suggest that the Utica and Trenton were at one time much more deeply buried than at the present (Moyer, 1982).

Whole rock iron analyses of non-ferroan regional dolomites also show an iron enrichment within a few feet of the top of the formation. Petrographic relations show that this is due to a late stage of iron sulfide formation which followed dolomitization. Also ferroan dolomite occurs as a late void lining in some samples. If as proposed earlier, the regional dolomite formed at or near the surface, the late addition of iron may have come from the overlying shale.

Whether or not the precursor limestone in the upper part of the Trenton acted as an internal source of iron is difficult to evaluate because presumably all Fe-rich limestone would now be dolomitized. However, several factors cast doubt on this idea. First, no mineralogic change (i.e., increase in clay content) which could account for an increase in iron content is observed in the limestone to cap dolomite transition. Also, no iron-rich calcite cements are found in grainstone portions of the Trenton. If the upper Trenton were Fe-rich at the time of deposition one might expect to observe late ferroan calcite cements in some samples. Detrital iron oxides and organic matter deposited with the Trenton probably contributed some Fe^{2+} to the formation of ferroan dolomite. However, it seems more likely that the source of much of the Fe^{2+} was external.

Source of Magnesium

Most of the Mg^{2+} needed for formation of the cap dolomite could be supplied by seawater. In the early stages of diagenesis, soon after deposition, seawater would be a major constituent of the sediment (30-70% of the total volume of lime mud). The Utica Shale would also contain large volumes of seawater, some of which could be expelled into the Trenton during compaction. Mg^{2+} contained in magnesian calcites could make a minor contribution to Mg^{2+} needed for formation of the cap dolomite. Irwin (1980) discusses the possibility of an organic source of Mg^{2+} in the formation of ferroan dolomite. Although the

importance of an organic source of Mg^{2+} is difficult to evaluate given present knowledge, it may be substantial in organic-rich sediments.

Carbon and Oxygen Isotopes of the Cap Dolomites

The ferroan cap dolomites are approximately 2.5-3.0°/oo depleted in ^{18}O when compared to Trenton limestones (Table 4). This again, may be due to: a) dolomitization associated with an influx of meteoric waters, or b) a temperature effect.

Petrographic evidence supports the contention that at least some of the cap dolomite formed after lithification. Also, the preservation of zoning in the cap dolomites suggests that they have not recrystallized to a large extent. The cap dolomites probably started to form within a few meters of the surface and continued to form during burial and compaction. Dolomitization would occur under conditions of slowly increasing temperature and $\delta^{18}O$ analyses of bulk samples represent an "average" of isotope ratios attained over a range of temperatures. This is supported by separation and analysis of two dolomitized fossil-matrix pairs from the cap dolomite. The course-grained ferroan dolomite which replaced fossils is in each case about 1°/oo depleted in ^{18}O when compared to the fine-grained matrix dolomite. This could be attributed to dolomitization at somewhat higher temperature. Two void filling ferroan dolomites were separated for isotope analysis and have $\delta^{18}O_{PDB}$ values of -7.8 and -9.9°/oo. This is also evidence that the formation of the cap dolomite occurred over a range of temperatures and depth.

Carbonate produced by modification of organic matter during burial diagenesis has varying $\delta^{13}C$ ratios which reflect the processes of sulfate reduction, fermentation, and decarboxylation (Claypool and Kaplan, 1974; Curtis, 1977; Irwin, et al., 1977; Irwin, 1980). These processes produce carbonate with characteristic light or heavy $\delta^{13}C$ ratios which are reflected in ferroan dolomite

concretions and cementstone horizons found in organic-rich shales (Irwin, et al., 1977; Irwin, 1980). The carbon isotope ratios of the cap dolomites of the Trenton Formation (Table 5) do not show the effects of these processes of organic matter decay, even though they may have formed over the same depth interval. This is due to the fact that in a limestone-water system the dominant carbon source is the rock ($\delta^{13}C_{PDB}$ = -1°/oo to +1°/oo) rather than pore solutions. Thus, during replacement of calcite by ferroan dolomite the $\delta^{13}C$ value of the dolomite will largely reflect the $\delta^{13}C$ of the precursor calcite. This along with the averaging effect of whole rock analyses can explain why the ferroan cap dolomite has $\delta^{13}C$ similar to Trenton limestones.

Models for the Origin of the Cap Dolomite

A number of models for the origin of the cap dolomites have been discussed in the past. Landes (1946) proposed that fluids rising along large fracture zones such as the Albion-Scipio, spread at the Trenton-Utica contact and formed the cap dolomite. In addition to hydrologic problems associated with this model, the cap and fracture dolomites have distinctly different chemistries and petrographic observations indicate that the fracture dolomite formed after the cap dolomite. It has also been suggested that an iron-rich soil horizon may have formed at the top of the Trenton prior to deposition of the Utica Shale and served as a source of Fe^{2+} during formation of the cap dolomite. No evidence of such a soil was observed in the southern part of the basin. However, it could be argued that this evidence was lost during diagenesis and dolomitization. In the center of the basin, where exposure did not occur ferroan dolomite is present and high concentrations of iron occur in the upper Trenton. Clearly, the source of iron in the upper Trenton is not related to the proposed unconformity and therefore not to the development of an iron-rich soil.

Preferred Model

In the model presented here, the precipitation of iron sulfide limits the precipitation of ferroan dolomite. The abundance of ferroan dolomite and distribution of the cap dolomite is therefore controlled by the availability of dissolved S^{2-} species during diagenesis.

The precipitation of iron sulfide has been shown to limit or preclude the precipitation of siderite (Berner, 1964, 1970, 1971, 1981; Curtis and Spears, 1967). In a system with abundant dissolved sulfide, pyrite or iron monosulfides will precipitate first. Siderite will not form until the dissolved sulfide concentration is lowered to a point where iron sulfides are no longer forming. This relationship has been observed both experimentally and in nature. It has been suggested that iron sulfide formation may exert a similar control on precipitation of ferroan dolomite (Irwin, 1980). Fe^{2+} substitutes for Mg^{2+} in ferroan dolomite and effectively reduces the Mg/Ca ratio needed for dolomitization. Thus, it is possible for a system to be supersaturated with respect to ferroan dolomite but undersaturated with respect to non-ferroan dolomite. If Fe^{2+} is being withdrawn by the precipitation of iron sulfides, the activity of Fe^{2+} may be lowered and drive the system out of the ferroan dolomite stability field. Only after dissolved sulfide concentrations are lowered and iron sulfide precipitation has ceased will Fe^{2+} concentrate in solution and ferroan dolomite precipitate.

In organic-rich sediments SO_4^{2-} is effectively removed from the pore water system by bacterial reduction to sulfide, the product being H_2S. Berner (1981) has pointed out that if abundant reduced iron is present, all available H_2S will be precipitated as iron sulfide. At depth sulfate reduction ceases to operate. If sources of Fe^{2+} and Mn^{2+} are still available these ions will concentrate in solution and later precipitate as carbonates.

Diagenesis of the upper portion of the Trenton Formation and the lower Utica Shale may be analagous to the situation described above. Figure 14 summarizes a model for the origin of the cap dolomite. In the southern and northern parts of the basin the Trenton appears to have been exposed prior to deposition of the overlying shale (Figure 14a). This period of exposure may have led to: a) the establishment of a freshwater lense in the upper Trenton, and/or b) mixing of interstitial seawater with freshwater either before or after deposition of the shale. The SO_4^{2-} concentration of freshwater is typically very low and subsequent sulfate reduction results in production of a limited amount of H_2S (Figure 14b). A small amount of iron sulfide forms depleting the system in dissolved sulfide. Fe^{2+} then concentrates in solution and is available to form abundant ferroan dolomite. Because of the fact that very little Fe^{2+} was precipitated in the form of iron sulfide, a ferroan dolomite cap was produced (Figure 14c).

In the central portion of the basin, subaerial exposure of the Trenton prior to deposition of the Utica Shale did not occur. Interstitial waters in both the shale and limestone would be Ordovician seawater containing abundant dissolved SO_4^{2-} (Figure 14d). Bacterial sulfate reduction would generate relatively large amounts of H_2S resulting in precipitation of abundant iron sulfides (Figure 14d). At depth, after the end of sulfate reduction and the depletion of dissolved sulfide, Fe^{2+} was able to concentrate in solution and ferroan dolomite formed (Figure 14e). A relatively small amount of ferroan dolomite formed because of the demands on the Fe^{2+} supply during precipitation of iron sulfide (Figure 14f).

The simplified model presented above is consistent with both the distribution of ferroan dolomite and the proportions of iron sulfide and ferroan dolomite observed in different parts of the basin. The iron sulfide phases present can be used to test this model. A combination of pyrite and iron monosulfide (possibly pyrrhotite) occurs in the basin center, both being relatively abundant

Figure 14. Model for the origin of the Trenton cap dolomite. See text for explanation.

BASIN MARGIN

A

Freshwater

Fresh or Brackish
Pore Fluids: low in SO_4^{2-}

seawater

Trenton Ls.

B

$\left[\begin{array}{l} \text{Sulfate Reduction Produces} \\ \text{Limited } H_2S \end{array} \right]$

seawater

Utica Sh.

Fe^{2+}

$H_2S \longrightarrow Fe\text{-sulfides} \longleftarrow Fe^{2+}$
form

Trenton Ls.

C

$\left[\begin{array}{l} \text{Sulfate Reduction} \\ \text{Ended in Trenton} \end{array} \right]$

Utica Sh.

Ferroan Dolomite
forms

Fe^{2+}, Mn^{2+}

Cap Dolomite

Figure 14.

BASIN CENTER

D

$$\left[\begin{array}{c}\text{Sulfate Reduction Produces}\\ \text{Abundant } H_2S\end{array}\right]$$

seawater

Utica Sh.

$H_2S \longrightarrow$ Fe – sulfides $\longleftarrow$ Fe^{2+}
form

Trenton Ls.

E

seawater

$$\left[\begin{array}{c}\text{Sulfate Reduction}\\ \text{Ended in Trenton}\end{array}\right]$$

Utica Sh.

Ferroan Dolomite
forms

Fe^{2+}, Mn^{2+}

Trenton Ls.

F

Utica Sh.

Ls. with Fe – sulfides
& Ferroan Dolomite

Trenton Ls.
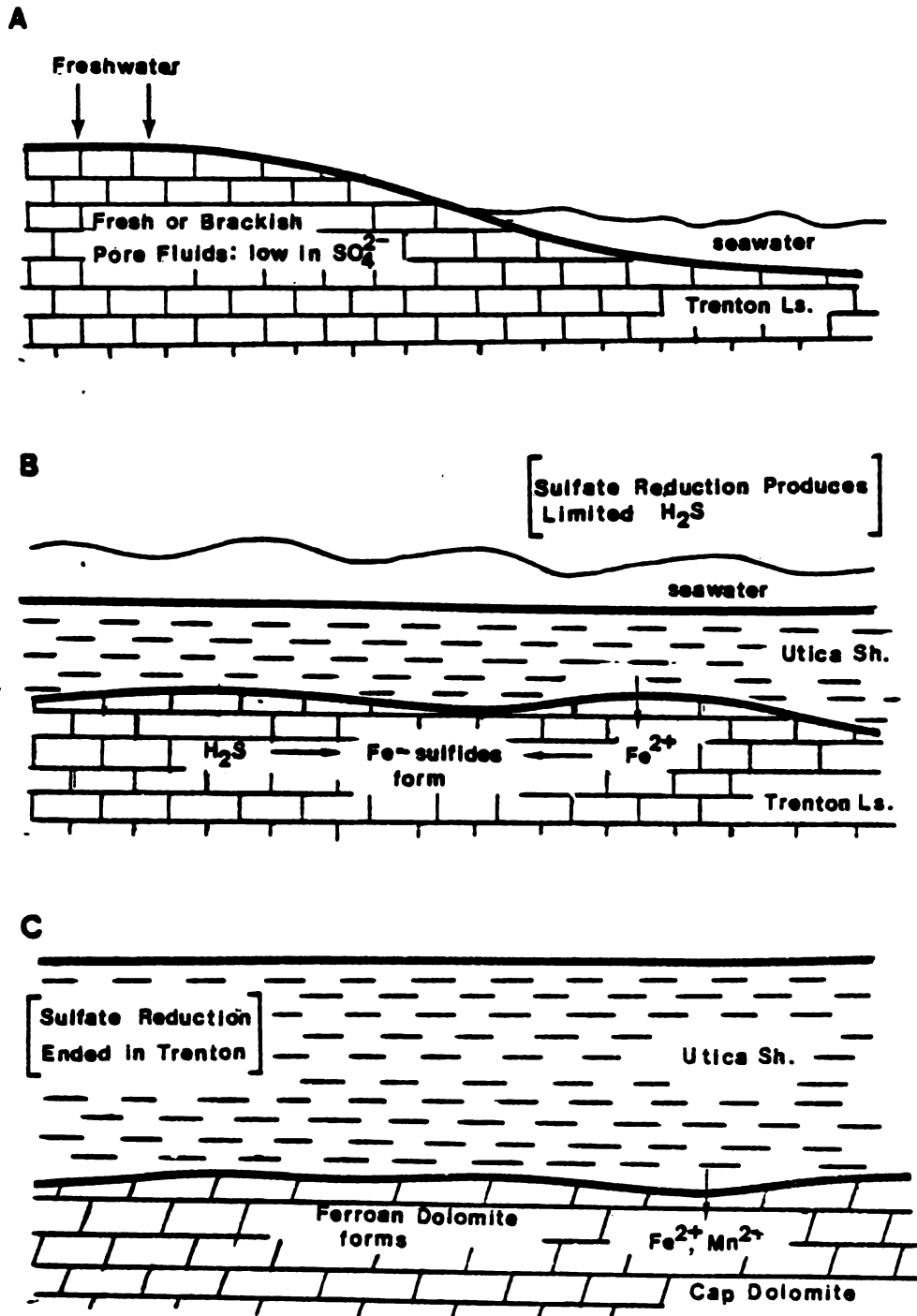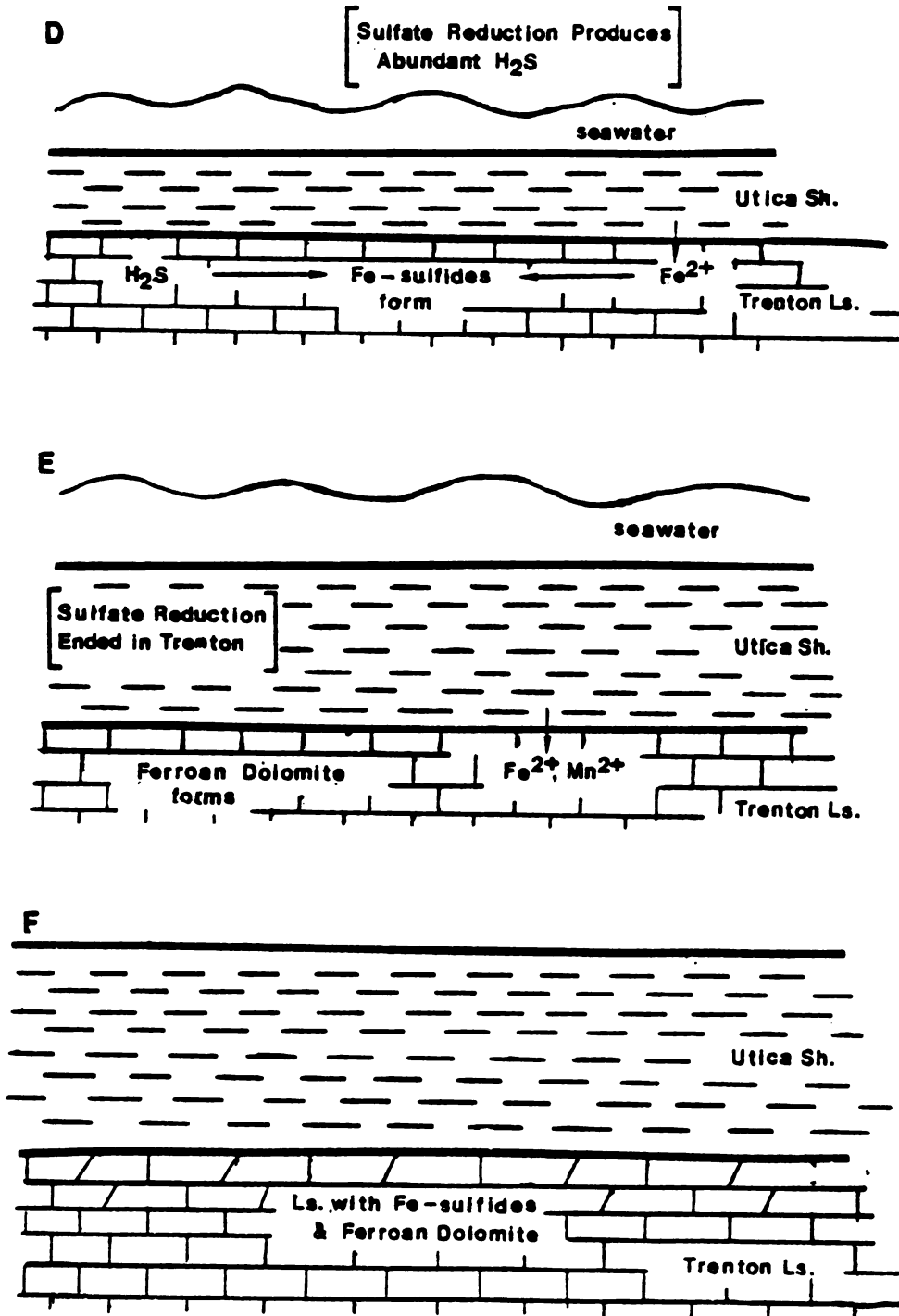
Figure 14 (Continued).

(Table 7). Iron sulfides in the cap dolomite occur in trace amounts and are primarily iron monosulfide (Table 7) with minor pyrite (observed petrographically). Berner, et al. (1979) and Berner (1981) suggest that a combination of pyrite and iron monosulfide would be present in sediments which become "sulfide limited" and later precipitate iron carbonate. If excess sulfide were available, iron monosulfides would presumably convert to pyrite. The abundance of pyrite in samples from the basin center, therefore, attests to the greater concentration of dissolved sulfide during diagenesis. The fact that the iron sulfide phase in the cap dolomite unit is almost entirely iron monosulfide indicates that the system was limited with respect to sulfide as a result of the influence of freshwater.

It might be expected that the ferroan cap dolomite would show the effects of meteoric freshwater and have more negative $\delta^{18}O$ values than ferroan dolomites from the basin center. This is not the case; in fact, ferroan dolomites from the basin center have slightly more negative ratios than cap dolomites. However, the isotopic influence of meteoric water in the cap dolomite would not be seen in this comparison if ferroan dolomite in the basin center formed at approximately $10^{\circ}C$ higher than the cap. This is not unreasonable in that the Trenton is presently much more deeply buried (5000-6000 feet) in the basin center, and the entire formation was more deeply buried in the past. Using a low geothermal gradient ($0.6^{\circ}C/100$ feet) this increase in temperature requires a burial difference of only 1600 feet.

CONCLUSIONS

1) Three major types of dolomite occur in the Ordovician Trenton Formation of the Michigan Basin. These dolomite types can be separated and recognized on the basis of their distribution in the basin, rock texture, $FeCO_3$ content, and $\delta^{18}O$ signatures.

Table 7. Electron microprobe analyses of iron sulfide phases
from the Trenton Formation.

Sample	Mineralogy	Wt%Fe	Wt%S
Cap			
E1-3651	Fe-monosulfide	55.0	45.0
		57.8	42.2
		53.9	46.0
JF 6101/5		53.2	46.8
		54.3	45.6
E1-3653		54.5	45.5
		54.7	45.3
		55.1	44.9
Basin Center			
ST 9904-4A	Pyrite	46.5	53.5
		47.3	52.7
		46.2	53.8
		47.4	52.6
		45.6	54.4
	Fe-monosulfide	54.5	45.5
		55.1	44.9
ST 9904/5	Pyrite	47.6	52.4
		46.4	53.6
	Fe-monosulfide	53.1	46.9
DT		54.7	45.3
		54.1	45.9
		52.5	47.5

2) The chemical differences clearly show that the three types of dolomite are genetically unrelated and represent three distinct dolomitization events. Petrographic relations indicate that Trenton dolomites formed in the order: a) regional dolomite, b) cap dolomite, and c) fracture dolomite.

3) Regional dolomites probably formed at or near the surface during early diagenesis. The $\delta^{18}O$ ratios of the regional dolomites are depleted when compared to adjacent limestones. This may indicate either dolomitization in a mixing-zone or recrystallization at elevated temperatures during burial.

4) Fracture-related dolomites formed after lithification and are most likely epigenetic in origin. This is supported by their distribution, textures, and very depleted $\delta^{18}O$ values. An estimated temperature of precipitation for baroque dolomite from the Albion-Scipio Field is approximately $80^{o}C$.

5) The Trenton cap dolomite is iron-rich and formed under reducing conditions. Ferroan cap dolomites probably began to form at shallow levels of burial and continued to form over a range of depth and temperature.

6) Ferroan dolomite occurs in the upper portion of the Trenton throughout the basin but forms a dolomite cap-rock unit only at the southern and northern edges of the basin. The most likely source of iron for the cap dolomite is the overlying Utica Shale.

7) The abundance of ferroan dolomite in the Trenton (therefore the distribution of the cap dolomite unit) was controlled by the availability of sulfide to form iron sulfides. The availability of sulfide was limited along the basin perimeter by subaerial exposure and influx of freshwater prior to deposition of the Utica Shale. This resulted in Fe^{2+} being available to form the ferroan cap dolomite. In the central portions of the basin, subaerial exposure did not occur and interstitial pore waters were seawater. The result was the precipitation of abundant iron sulfides and minor amounts of ferroan dolomite.

REFERENCES

Al-Shaieb, Z. and Shelton, J. W., 1978. Secondary ferroan dolomite rhombs in oil reservoirs, Chadra Sands, Gialo Field, Libya. Am. Assoc. Geol. Bull., v. 62, p. 463-468.

Ardrey, R. H., 1978. Diagenesis of the Trenton Limestone in the Northville oil field, Michigan (abst.). Geol. Soc. Am. Abstr. w/Programs, v. 10, no. 6, p. 245-246.

Badiozamani, K., 1973. The dorag dolomitization model - application to the Middle Ordovician of Wisconsin. Jour. Sed. Petrology, v. 43, p. 965-984.

Baker, P. A. and Kastner, M., 1981. Constraints on the formation of sedimentary dolomite. Science, v. 203, p. 214-216.

Berner, R. A., 1964. Stability fields of iron minerals in anaerobic sediments. Geochim. Cosmochim. Acta., v. 28, p. 1497-1503.

_____, 1970. Sedimentary pyrite formation. Am. Jour. Sci., v. 268, p. 1-23.

_____, 1971. Principles of Chemical Diagenesis. McGraw-Hill, N.Y., 240p.

_____, 1981. A new geochemical classification of sedimentary environments. Jour. Sed. Petrology, v. 51, p. 359-365.

Berner, R. A., Baldwin, T. and Holdren, G. R., 1979. Authigenic iron sulfides as paleosalinity indicators. Jour. Sed. Petrology, v. 49, p. 1346-1350.

Boles, J. R., 1978. Active ankerite cementation in the subsurface Eocene of southwest Texas. Contrib. Mineral. Petrol., v. 68, p. 13-22.

Boles, J. R. and Franks, S. G., 1979. Clay diagenesis in Wilcox Sandstones of southwest Texas: Implications of smectite diagenesis on sandstone cementation. Jour. Sed. Petrology, v. 49, p. 55-70.

Brand, U. and Veizer, J., 1981. Chemical diagenesis of a multicomponent carbonate system - 2: Stable isotopes. Jour. Sed. Petrology, v. 51, p. 987-997.

Brand, U., 1982. The oxygen and carbon isotope composition of carboniferous fossil components: sea water effects. Sedimentology, v. 29, p. 139-147.

Burst, J. F., 1969. Diagenesis of Gulf Coast clayey sediments and its possible relation to petroleum migration. Am. Assoc. Petrol. Geol., v. 53, p. 73-93.

Carpenter, A. B., 1980. The chemistry of dolomite formation I: The stability of dolomite. SEPM Spec. Pub. no. 28, p. 111-121.

Carroll, D., 1958. Role of clay minerals in the transportation of iron. Geochim. Cosmochim. Acta., v. 14, p. 21-26.

Choquette, P. W., 1971. Late ferroan dolomite cement, Mississippian carbonates, Illinois Basin, USA: In O. P. Bricker (ed.), Carbonate Cements. Johns Hopkins Univ. Press, Baltimore, MD, p. 339-346.

Claypool, G. E. and Kaplan, I. R., 1974. The origin and distribution of methane in marine sediments. In I. R. Kaplan (ed.), Natural Gases in Marine Sediments. Plenum, N.Y., p. 99-139.

Clayton, R. N., Friedman, I., Graf, D. L., Mayeda, T. K., Meents, W. F. and Shimp, N. F., 1966. The origin of saline formation waters: I. Isotopic composition. Jour. Geophys. Res., v. 71, p. 3869-3882.

Cohee, G. V., 1948. Cambrian and Ordovician rocks in the Michigan Basin and adjoining areas. Am. Assoc. Petrol. Geol., v. 32, p. 1417-1448.

Curtis, C. D. and Spears, D. A., 1968. The formation of sedimentary iron minerals. Econ. Geol., v. 63, p. 257-262.

Curtis, C. D., 1967. Diagenetic iron minerals in some British carboniferous sediments. Geochim. Cosmochim. Acta., v. 31, p. 2109-2123.

_____, 1978. Possible links between sandstone diagenesis and depth-related geochemical reactions occurring in enclosing mudstones. Geol. Soc. Lond. Jour., v. 135, p. 107-117.

Degens, E. T. and Epstein, S., 1964. Oxygen and carbon isotope ratios in coexisting calcites and dolomites from recent and ancient sediments. Geochim. Cosmochim. Acta., v. 28, p. 23-44.

Dickson, J. A. D. and Coleman, M. L., 1980. Changes in carbon and oxygen isotope composition during limestone diagenesis. Sedimentology, v. 27, p. 107-118.

Drever, J. L., 1971. Magnesium-iron replacement in clay minerals in anoxic marine sediments. Science, v. 172, p. 1334-1336.

Ells, G. D., 1969. Architecture of the Michigan Basin. Mich. Basin Geol. Soc. Ann. Field Excur., p. 60-88.

Fisher, J. H., 1969. Early Paleozoic history of the Michigan Basin. Mich. Basin Geol. Soc. Ann. Field Excur., p. 89-93.

Folk, R. L. and Assereto, R., 1974. Giant aragonite rays and baroque white dolomite in tepee-fillings, Triassic of Lombardy, Italy (abstr.). Am. Assoc. Petrol. Geol., Abstr. w/Programs, Ann. Mtg., San Antonio, p. 34-35.

Frank, J. R., 1981. Dedolomitization in the Taum Sauk Limestone (Upper Cambrian), southeast Missouri. Jour. Sed. Petrology, v. 51, p. 7-18.

Fritz, P., 1971. Geochemical characteristics of dolomites and the $\delta^{18}O$ content of Middle Devonian oceans. Earth Planet. Sci. Lett., v. 11, p. 277-282.

Garrels, R. M. and Christ, C. L., 1965. Solutions, Minerals, and Equilibria. Harper and Row, New York, 450p.

Goldsmith, J. R. and Graf, D. L., 1958. Structural and compositional variations in some natural dolomites. Jour. Geol., v. 66, p. 678-692.

Goldsmith, J. R., Graf, D. L., Witters, J. and Northrup, D. A., 1962. Studies in the system $CaCO_3$-$MgCO_3$-$FeCO_3$: 1. Phase relations, 2. A method for major element spectochemical analysis, 3. Composition of some ferroan dolomites. Jour. Geol., v. 70, p. 659-688.

Gregg, J. M., 1982. The origin of xenotopic dolomite texture. Ph.D. Dissertation, Michigan State Univ.

Hinze, W. J. and Merritt, D. W., 1969. Basement rocks of the southern peninsula of Michigan. Mich. Basin Geol. Soc. Ann. Field Excur., p. 28-59.

Hinze, W. J., Kellogg, R. L. and O'Hara, N. W., 1975. Geophysical studies of basement geology of southern peninsula of Michigan. Am. Assoc. Petrol. Geol., v. 59, p. 1562-1584.

Heller-Kallai, L. and Rozenson, I., 1978. Removal of magnesium from interstitial waters in reducing environments: the problem reconsidered. Geochim. Cosmochim. Acta., v. 42, p. 1907-1909.

Irwin, H., Curtis, C. D. and Coleman, M., 1977. Isotopic evidence for source of diagenetic carbonates formed during burial of organic-rich sediments. Nature, v. 269, p. 209-213.

Irwin, H., 1980. Early diagenetic precipitation and pore fluid migration in the Kimmeridge clay of Dorset, England. Sedimentology, v. 27, p. 577-591.

Land, L. S. and Dutton, S. P., 1978. Cementation of a Pennsylvanian deltaic sandstone: Isotopic data. Jour. Sed. Petrology, v. 48, p. 1167-1176.

Land, L. S., 1980. The isotopic and trace element geochemistry of dolomite: the state of the art. SEPM Spec. Pub. no. 28, p. 87-110.

Landes, K. K., 1946. Porosity through dolomitization. Am. Assoc. Petrol. Geol., v. 30, p. 305-318.

Lilienthal, R. T., 1978. Stratigraphic cross sections of the Michigan Basin. Mich. Geol. Surv., Rept. Invest. no. 19.

Lowenstam, H. A., 1961. Mineralogy, O^{18}/O^{16} ratios, and strontium and magnesium contents of Recent and fossil brachiopods and their bearing on the history of the oceans. Jour. Geol., v. 69, p. 241-260.

Margara, K., 1974. Compaction, ion formation, and osmosis in shale and their significance in primary migration. Am. Assoc. Petrol. Geol., v. 58, p. 283-290.

Matsumoto, R. and Iijima, A., 1981. Origin and diagenetic evolution of Ca-Mg-Fe carbonates in some coal fields of Japan. Sedimentology, v. 28, p. 239-259.

Mattes, B. W. and Mountjoy, E. W., 1980. Burial dolomitization of the Upper Devonian Miette Buildup, Jasper National Park, Alberta. SEPM Spec. Publ. no. 28, p. 259-297.

Matthews, A. and Katz, A., 1977. Oxygen isotope fractionation during dolomitization of calcium carbonate. Geochim. Cosmochim. Acta., v. 41, p. 1431-1438.

McKenzie, J. A., 1981. Holocene dolomitization of calcium carbonate sediments from the coastal sabkhas of Abu Dhabi, U.A.E.: a stable isotope study. Jour. Geol., v. 89, p. 185-198.

Mesher, P. K., 1980. Structural evolution of SE Michigan - Middle Ordovician to Middle Silurian. Unpub. M.S. Thesis, Michigan State Univ.

Mossler, J. H., 1971. Diagenesis and dolomitization of Swope Formation (Upper Pennsylvanian) southeast Kansas. Jour. Sed. Petrology, v. 41, p. 962-970.

Moyer, R. B., 1982. Thermal maturity and organic content of selected Paleozoic formations - Michigan Basin. Unpub. M.S. Thesis, Michigan State Univ.

M'Rabet, A., 1981. Differentiation of environments of dolomite formation, Lower Cretaceous of central Tunisia. Sedimentology, v. 28, p. 331-352.

Murata, K. J., Freidman, I. and Cremer, M., 1972. Geochemistry of diagenetic dolomites in Miocene marine formations of California and Oregon. U.S. Geol. Surv. Prof. Paper 724-C, 12p.

Nash, A. J. and Pittman, E. D., 1975. Ferro-magnesian calcite cement in sandstones. Jour. Sed. Petrology, v. 45, p. 258-265.

Newhart, R. E., 1976. Carbonate facies in the Middle Ordovician, Michigan Basin. Unpub. M.S. Thesis, Michigan State Univ.

Northrup, D. A. and Clayton, R. N., 1966. Oxygen isotope fractionations in systems containing dolomite. Jour. Geol., v. 74, p. 174-196.

Nurmi, R. D., 1972. Upper Ordovician stratigraphy of the southern peninsula of Michigan. Unpub. M.S. Thesis, Michigan State Univ.

O'Neil, J. R., Clayton, R. N. and Mayeda, T. K., 1969. Oxygen isotope exchange between divalent metal carbonates. Jour. Chem. Phys., v. 51, p. 5547-5558.

Perry, E. C., Jr. and Tan, F. C., 1972. Significance of oxygen and carbon isotope variations in Early Precambrian cherts and carbonate rocks of southern Africa. Geol. Soc. Amer. Bull., v. 83, p. 647-664.

Radke, B. M. and Mathis, R. L., 1980. On the formation and occurrence of saddle dolomite. Jour. Sed. Petrology, v. 50, p. 1149-1168.

Rooney, L. F., 1966. Evidence of unconformity at the top of Trenton Limestone in Indiana and adjacent states. Am. Assoc. Petrol. Geol., v. 50, p. 533-546.

Rosenberg, P. E., 1967. Subsolidus relations in the system $CaCO_3$-$MgCO_3$-$FeCO_3$ between 350 and 550°C. Am. Mineral., v. 52, p. 787-796.

Rosenberg, P. E. and Foit, F. F., Jr., 1979. The stability of transition metal dolomites in carbonate systems: a discussion. Geochim. Cosmochim. Acta., v. 43, p. 951-955.

Sharma, T. and Clayton, R. N., 1965. Measurement of $^{18}O/^{16}O$ ratios of total oxygen from carbonates. Geochim. Cosmochim. Acta., v. 29, p. 1347-1354.

Shaw, H. R., 1959. Mineralogical studies in the Bunker Hill Mine, Idaho. Ph.D. Thesis, Univ. of California (Berkley).

Shaw, B., 1975. Geology of the Albion-Scipio Trend, southern Michigan. Unpub. M.S. Thesis, Univ. of Michigan, 63p.

Veizer, J. and Hoefs, J., 1976. The nature of O^{18}/O^{16} and C^{13}/C^{12} secular trends in sedimentary carbonate rocks. Geochim. Cosmochim. Acta., v. 40, p. 1387-1395.

Wanless, H. R., 1979. Limestone response to stress: pressure solution and dolomitization. Jour. Sed. Petrology, v. 49, p. 437-462.

Wong, P. K. and Oldershaw, A., 1981. Burial cementation in the Devonian Kaybob Reef Complex, Alberta, Canada. Jour. Sed. Petrology, v. 51, p. 507-520.